SCHOOL OF ELECTRONIC, ELECTRICAL AND COMPUER ENGINEERING

THE UNIVERSITY
OF BIRMINGHAM

INVESTIGATION OF MICROWAVE TRI-RESONATOR STRUCTURES

Negassa Sori Gerba

A thesis submitted to the University of Birmingham for the degree of Master of Research in Electronic, Electrical and Computer Engineering

April 2012

Abstract

In this thesis a clear synthesis technique to design a power splitter based on three resonators is introduced. A new analytic synthesis method is developed to investigate a coupled resonator structure with only three resonators and three ports. The general formulae to calculate the coupling coefficients between resonators are analytically derived. This method avoids the use of the polynomial synthesis technique.

The mathematical analysis is extended for the realisation of an asymmetric frequency response of a trisection filter. A simple mathematical function with a minimum number of parameters is developed which can be used as a cost function when using optimisation. These parameters are coupling coefficients and external quality factors, and are called control variables. A coupling matrix optimisation technique is used to obtain optimised values of control variables to realise an asymmetric frequency response of a trisection filter. The optimisation algorithms effectively reduce the cost function, and generate appropriate values of control variables when the function is minimised.

Acknowledgments

Having completed this thesis, I thank the Almighty GOD for keeping me in good health to accomplish the assignments that were expected of me in this thesis.

During my M.Res study at the University of Birmingham, I have been privileged to have Professor Mike Lancaster as my supervisor. I would like to thank him for proving me an opportunity to conduct this M.Res research. I am grateful to him for his patient mentoring, inspiring suggestions and endless editing.

My deepest gratitude also goes to my wife for her all round support and encouragement she has provided me throughout the year while studying my M.Res research. She has endured much sacrifice for the sake of my education. I could not have accomplished what I did without her boundless love, sacrifice, support, and encouragement.

I would like to extend my thanks to my peers in the Emerging Device Technology (EDT) research group in general and Dr. Xiobang Shang in particular for providing discussions on technical issues and suggestions that has always been granted without any hesitation.

Last, but not least, my acknowledgments also goes to UK-Council for Assisting Refugee Academics (CARA) for covering the cost of my M.Res study.

Dedicated To my Wife

(Genet D Merera)

And

My Children

(Simeera and Hawwera)

Table of Contents

Chapter 1

Introduction

1.1. Background

This review considers methods of calculating coupling matrix and external quality factors for a coupled resonator filter with multiple ports. Multiport microwave coupled resonator synthesis has been presented in [11], in addition the two port formulation for *n*-coupled resonator filter for both electrically and magnetically coupled resonators has also been implemented in [1]. In the literature, different methods have been used to extract the coupling matrix and external quality factors for multi port networks [8]. Coupling matrix methods of synthesising microwave filters are discussed in chapter 4. For a two-port network, an optimisation procedure utilizing a mathematical function for the extraction of coupling coefficients and external quality factors has been proposed in [19].

In the literature, several approaches [1], [2], [11], [12], [17] have been proposed to realise the frequency response of coupled resonators for different resonator structures. General tri-resonator filters and their capability of providing both bandpass and band-reject behaviour has been investigated in [10], however, to my knowledge, the tri-resonator structure has not been investigated in detail.

The proposed equivalent circuit of a tri-resonator structure is shown in Figure 1.1. The circuit demonstrate the coupling between adjacent and non-adjacent resonators. A general coupling theory of resonator circuits and their applications are presented in Chapter 3.

Even though a large number of articles dealing with coupling matrix synthesis have recently been and being published [8], [11], [12], [17], [18], none of them go into details about how to calculate the coupling parameters of a three port network with only three resonators by analytic method.

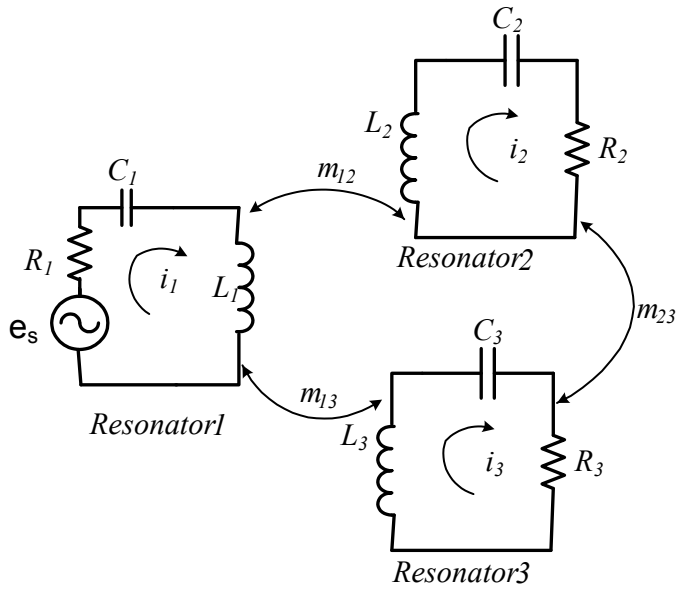

Figure 1.1 Equivalent circuit prototype of Tri-resonator filter structure.

In this thesis, for the realisation of a tri-resonator structure, the values of normalised coupling coefficients and external quality factors that can realise a required response is to be calculated analytically. This is attempted without recourse to polynomials.

1.2. Overview of Power Splitter

A power splitter is a three port network that splits incoming signals from an input port into two paths or channels, dependent on frequency. It is used in multiport networks for the transmission and reception of signals or channel separation. Power splitters are an RF microwave accessory constructed with equivalent (often 50Ω) resistance at each port. These components divide power of a uniform transmission line equally between ports.

They provide a good impedance match at both the output ports when the input is terminated in the system characteristic impedance (usually 50Ω). Once a good source match has been achieved, a power splitter can be used to divide the output into equal signals.

1.3. Thesis Overview

By investigating a three resonator structure, looking at the coupling coefficients between the resonators, simple power splitters are to be investigated. The investigation is based on the radio frequency (RF) circuit analysis and coupling matrix optimisation techniques to make the response of coupled tri-resonator structure close to the idealised circuit responses of the power splitters. The work in this thesis also covers the theory and design of trisection filter for two-port tri-coupled resonators.

Determination of coupling matrix, $[m]$ and external quality factors, $[q_{ei}]$ for $i = 1,\ 2,\ 3$ of the three resonators by analytic and coupling matrix optimisation techniques are the main challenging aspect of this thesis. The thesis will try and determine what specifications of power splitters are possible with only three resonators.

1.4. Thesis Motivation

There has been an increasing demand in reducing design complexity of microwave components. The thesis addresses the method to calculate the normalised coupling coefficients and external quality factors for the design of power splitter without the need to use optimisation or even polynomials. Thus, it will investigate and develop simple mathematical formulations to calculate the coupling parameters.

In this thesis, assumptions are made during a general 3×3 coupling matrix manipulation in developing mathematical relations between normalised coupling coefficients and external quality factors. The reflection zeros for the three port tri-coupled tri-resonator structures have been specified and used in the analytical equations to reduce the complexity of mathematical derivations. A 3 dB power splitter is designed using the calculated normalised coupling coefficients and external quality factors. For the trisection filter, a general equation with minimum number of parameters to be optimised is developed from the transmission and reflection scattering parameters. The mathematical relation developed has only 4 parameters rather than 12 for the full solution. Thus, optimisation algorithms are only required for four variables.

1.5. Thesis Outline

The organisation of this thesis is as follows:

After the introduction in Chapter 1, chapter 2 looks in to the basics of the microwave resonators. In this chapter, the basic operations of microwave resonators are briefly discussed by using lumped resonant circuits. The loaded and unloaded quality factors of microwave resonators are also discussed briefly.

Chapter 3 describes coupled resonator circuits in conjunction with the coupling theory of coupled resonators. A detailed derivation of a general 3×3 coupling matrix of tri-coupled resonators with a three-port network, which will be used in the rest of the thesis, is presented. A combined relation for the transmission and reflection scattering parameters are drawn from loop and node equation formulations for magnetically and electrically coupled resonator circuits, respectively. Cross couplings and direct couplings are discussed in this chapter to present them in coupling matrix synthesis which is also

covered here. A circuit prototype model for the tri-resonator structure and the proposed coupling structure for the design of power splitter and for the realisation of trisection filter are demonstrated.

Passive microwave filters such as power splitter theories are presented in chapter 4. The basics of polynomial synthesis for the two ports and three ports network are briefly introduced. Coupling matrix method for designing filters is discussed in detail. Lastly in this chapter, detailed mathematical analysis is carried out to derive mathematical formulae to calculate transmission and reflection zero locations for the proposed structure.

Chapter 5 describes an analytical design method for tri-resonator power splitters. This section mainly focuses on developing the analytical design by calculating normalised coupling coefficients and the scaled external quality factors. A general analysis of the power splitter is presented, which is to develop a general equation for calculating the normalised coupling coefficients and the external quality factors of resonators. In deriving the general formulae, some assumptions are made to simplify the design. To develop a general formulae, the frequency locations of reflection zeros are specified and used throughout mathematical analysis to reduce the complexity. Specifying the frequency locations of reflection zeros, and using them in the general formulae will also reduce the number of unknown parameters within the equations. A design of a trisection filter can be achieved by extending this equation; however, in this case optimisation methods are used as it is not possible to calculate all the required coupling parameters. It is worth mentioning here that the analytic approach has simplified the equation and reduces the time taken by the optimisation routine.

The final chapter of the thesis (chapter 6) presents the conclusions and suggested works. The significance and contribution of this thesis work is summarised in this Chapter.

Chapter 2

Microwave Resonators

2.1. Introduction

Resonators are lumped element networks or distributed circuits that allow the exchange of electric and magnetic energies with low loss. Lumped elements such as inductors and capacitors are usually employed for resonators at frequencies below 300 Megahertz (MHz) [3]. At higher frequencies, the dimensions of the general lumped elements are comparable to the wavelength in size. Smaller devices are possible with the advantage of integrated circuit (IC) technology. However, small sizes result in poor power handling capacity and low quality factors, and this is presented in the subsequent sections. Therefore, resonators consisting of distributed components are usually constructed for applications in the microwave frequency range. Distributed resonator circuits utilize the resonant properties of standing waves and thus are generally of a size comparable to wavelength. Although lumped circuits are not generally applicable at high frequencies, they are good models to present the basic operation of all resonators.

In this chapter lumped resonant circuits and microstrip ring resonators are discussed. Ring resonators can be easily cross coupled with the wide range of coupling coefficients between resonators. This is presented in chapter 5 for the practical design of tri-resonator power splitter and trisection filter.

2.2. Lumped Resonant Circuits

A resonant circuit or tuned circuit consists of an inductor, L, a capacitor, C and a resistor, R in series or parallel. When connected together, they can act as an electrical resonator storing electrical energy oscillating at the circuits' resonant frequency.

RLC circuits are used in the generation of signals at a particular frequency, or picking out a signal at a particular frequency from more complex filters. They are key components in many applications such as oscillators, filters, tuners and frequency mixers. An LC circuit is an idealized model since it assumes there is no dissipation of energy due to resistance. The purpose of an RLC circuit is to oscillate with minimal damping, and for this reason their resistance is made as low as possible. Even though there is no practical circuit, which is without losses, it is instructive to study this pure form to gain a good understanding. A parallel and series RLC lumped element resonator circuits are shown in figure 2.1(a) and (b) respectively.

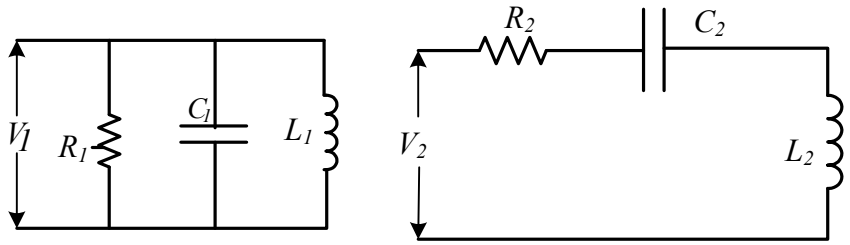

Figure 2.1 Resonant circuits (a) parallel and (b) series

Consider the simple parallel resonant circuit shown in figure 2.1 (a). In this case, lumped elements R_1, C_1 and L_1 share a common voltage V_1. If P_{loss} is the average power loss in the resistor R_1, W_m the average magnetic energy in the inductor L_1 and W_e the average

electric energy stored in the capacitor C_1, the average dissipated power can be expressed as

$$P_{loss} = \frac{1}{2}\frac{|V_1|^2}{R_1} \tag{2.1}$$

Its input impedance is given by

$$Z = R_1 + j\omega L_1 + \frac{1}{j\omega C_1} \tag{2.2}$$

At the resonance the input impedance is purely real and equal to R_1. Resonance occurs when the stored average magnetic and electric energies are equal, such as $W_m = W_e$. The frequency at which resonance occurs is referred to as angular resonant frequency ω_0, which is defined as

$$\omega_0 = \frac{1}{\sqrt{L_1 C_1}} \tag{2.3}$$

An important parameter of a resonant circuit is its quality factor, Q and this is discussed in the following section briefly.

2.2.1. The Quality Factor, Q

The quality factor, Q is a useful measure of sharpness of resonance [3], and also it is used to measure the loss of resonator circuit. Q can be defined as

$$Q = \omega \frac{\text{time average energy stored in the system}}{\text{average energy loss per second in the system}}$$

As can be seen from this definition, low loss implies a higher quality factor, Q.

A high Q factor results in a steep roll-off and narrow bandwidth of the resonator [7] as shown in figure 2.2. At resonance, Q can be expressed in terms of the magnetic and electric energies stored in lumped element resonators as well as microwave resonators as [7]

$$Q = \omega_0 \frac{W_m + W_e}{P_{loss}} \tag{2.4}$$

In terms of lumped resonant circuit elements R_1, C_1 and L_1, the Q of the parallel resonant circuit can be evaluated as

$$Q = \omega_0 R_1 C_1 = \frac{R_1}{\omega_0 L_1} \tag{2.5}$$

Thus it can be seen from equation (2.5) that a small value of resistance in an RLC circuit implies low Q-factor.

Q-factor can also be defined in terms of resonance frequency ω_0 and bandwidth $\Delta\omega$ of the response of the resonator circuit as

$$Q = \frac{\omega_0}{\Delta\omega} = \frac{\omega_0}{\omega_2 - \omega_1} \tag{2.6}$$

where ω_0 is the angular resonant frequency and $\Delta\omega = \omega_2 - \omega_1$ is the 3-dB bandwidth

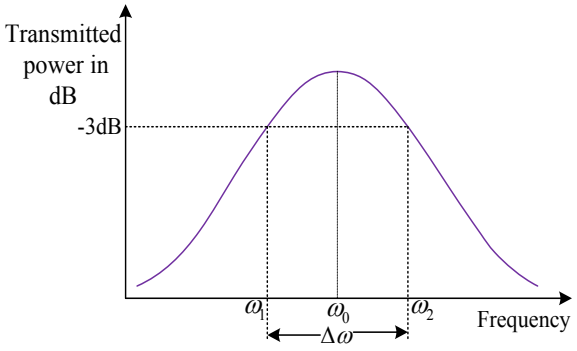

Figure 2.2 Graph of Q-factor

2.2.1.1. Loaded and Unloaded Quality Factor, Q

The quality factor defined in the previous section is in the absence of any loading effects caused by external circuitry, and it is the characteristic of the resonant circuit itself and is called unloaded Q_u. The unloaded quality factor, Q_u involves the power loss by resonant circuit only. In practice, a resonant circuit is coupled to external circuitry, which dissipates additional power denoted by P_e. The external Q factor denoted by Q_e is defined in terms of the power dissipated in the external circuitry, and magnetic energy, W_m and electric energy, W_e stored in inductor L_1 and capacitor C_1 respectively as

$$Q_e = \omega_0 \frac{W_m + W_e}{P_e} \tag{2.7}$$

Similarly, the Q factor of the loaded resonator, Q_L associated with the total loss can be expressed as

$$Q_L = \omega_0 \frac{W_m + W_e}{P_{loss} + P_e} \tag{2.8}$$

Looking at equation (2.8), it is clear that the effect of the external load always lowers the overall Q factor of a resonator.

Using equations (2.4), (2.7) and (2.7), the relationship between Q_L, Q_u and Q_e can be shown as

$$\frac{1}{Q_L} = \frac{1}{Q_u} + \frac{1}{Q_e} \tag{2.9}$$

The degree of coupling between the external circuit and resonant circuit is measured by coupling coefficient k, and in general, k can be defined in terms of the Q factor as [7]

$$k = \frac{Q_u}{Q_e} \text{ or } k = \frac{Q_u - Q_L}{Q_L} \tag{2.10}$$

The coupling coefficient k denotes the ratio of the power dissipated in the external circuit to the power loss in the resonant circuit itself. For the condition k=1, the coupling is referred to as critical coupling. If k >1, the resonator is said to be over coupled and k<1 is called under coupled [9].

Chapter 3

Coupling of Resonator Circuits

3.1. Introduction

For the design of RF/microwave filters, coupling of resonator circuits is one of the most significant factors affecting filter performance. A set of microwave resonators electrically and/or magnetically coupled to each other and coupled to an external feed circuit are used to realize a filter. The number and the type of the couplings between the resonators determine the overall performance of the device [1]. Design techniques are extended in this thesis to a three-port network having a single input and two output port circuits such as a power splitter. The general coupling matrix of a two-port *n*-coupled resonator filter is formulated in detail in [1]. Based on the principle in [1], the general coupling matrix of a three-port tri-coupled resonator is derived, and its relation to the scattering parameters is presented in the next sections. For the design of power splitter, this thesis is mainly based on the general formulae of scattering parameters in terms of normalised coupling matrix derived in this section.

3.2. Back Ground Theory of Coupling

A general technique for designing coupled resonator filters is based on coupling coefficients of inter- coupled resonators and the external Q-factors of the input and output resonators [1].

The coupling coefficient, k, of two coupled microwave resonators as shown in figure 3.1

can be defined on the basis of the ratio of coupled energy to stored energy, and it can be defined mathematically as [1]

$$k_{12} = \frac{\iiint \varepsilon \underline{E_1} \bullet \underline{E_2} dv}{\sqrt{\iiint \varepsilon \left|\underline{E_1}\right|^2 dv \times \iiint \varepsilon \left|\underline{E_2}\right|^2 dv}} + \frac{\iiint \mu \underline{H_1} \bullet \underline{H_2} dv}{\sqrt{\iiint \mu \left|\underline{H_1}\right|^2 dv \times \iiint \mu \left|\underline{H_2}\right|^2 dv}} \tag{3.1}$$

where $\underline{E}_1$ and $\underline{E}_2$ are the electric fields in resonator 1 and 2, respectively, and $\underline{H}_1$ and $\underline{H}_2$ are the magnetic fields in resonator 1 and 2, respectively.

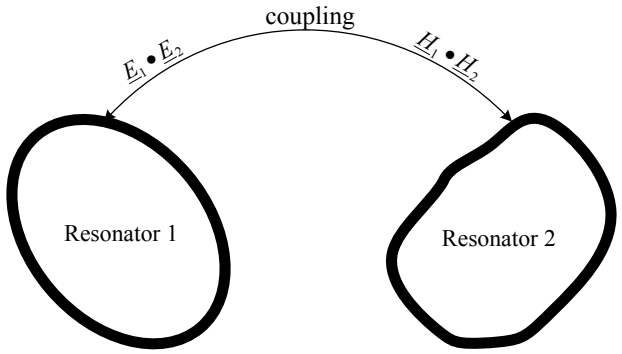

Figure 3.1 General coupled microwave resonators where resonators 1 and 2 can have different structure and have different resonant frequencies [1].

Mathematically, the dot operation of the space vector describes the interaction of the coupled resonator as shown in equation (3.1). This allows the coupling to have either positive or negative sign. A positive sign would imply that the coupling enhances the stored energy of uncoupled resonators, whereas a negative sign indicates that coupling reduces the stored energy of uncoupled resonator. Therefore, the electric and magnetic coupling could either have same effect if they have the same sign, or have the opposite effect if their signs are opposite [1].

The typical resonant response of a coupled resonator is shown in figure 3.2. The magnitude of the coupling coefficient defines the separation *d* of the two resonance peaks as in Figure 3.2.

Normally, the stronger the coupling, the wider separation *d* of the two resonance peaks, and the deeper the trough is in the middle [1].

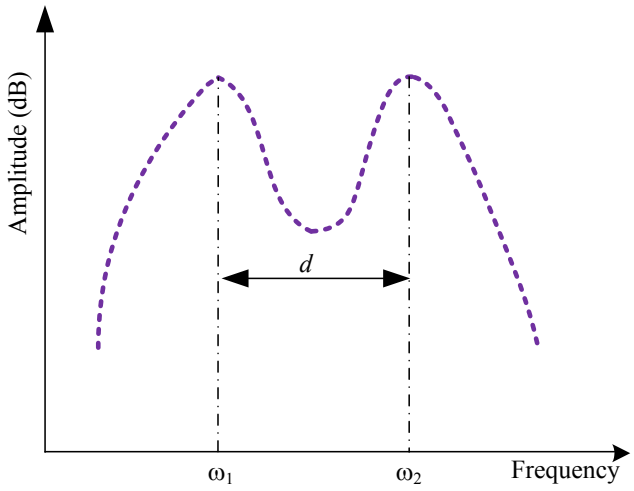

Figure 3.2 Resonant response of coupled resonator structure [1]

For a pair of synchronously tuned resonators, the coupling coefficient in terms of ω_1 and ω_2 is defined as in [31]

$$k = \pm \frac{\omega_2^2 - \omega_1^2}{\omega_2^2 + \omega_1^2} \tag{3.2}$$

where ω_1 and ω_2 are lower and upper cut-off angular frequencies, respectively.

As $\omega = 2\pi f$, equation (3.2) can be more simplified as

$$k = \pm \frac{f_2^2 - f_1^2}{f_2^2 + f_1^2} \tag{3.3}$$

Equation (3.3) can be used for both magnetic and electric coupling calculations [1], but the phase of S_{21} must be taken into account to get the sign of k. Magnetic and electric coupling of resonators will be discussed in the next section.

3.3. General 3×3 Coupling Matrix Derivation for Tri-resonator Structure

The equivalent circuit description for a three-port network of tri-coupled resonator structure is shown in figure 3.3. In the subsequent sections, the equivalent circuit of magnetically and electrically coupled resonators with only three resonators is considered in the derivation of a 3×3 coupling matrix. The reflection and transmission scattering parameters in terms of this coupling matrix for the magnetically coupled and electrically coupled resonators are also generalised and incorporated into one form.

3.3.1. Magnetic Coupling

Energy may be coupled between adjacent resonators by either an electric or a magnetic or both. Figure 3.3 shows the equivalent circuit of three resonators coupled to each other with mutual inductances linking each inductor.

The impedance matrix for magnetically *n*-coupled or the admittance matrix for electrically *n*- coupled resonators for the two port network is formulated in [2]. The coupling matrix of n - coupled resonators in an *N*-port network is obtained from the equivalent circuit of *n*-coupled resonators in [2]. A general normalised coupling matrix $[A]$ in terms of coupling coefficients and external quality factors for any coupled resonator structure with multiple outputs has been derived in [2]. Using loop equation formulation used in [1] for the magnetically coupled resonator, a normalised coupling matrix $[A]$ can be derived from a

tri-coupled tri-resonator structure shown in figure 3.3. Figure 3.3 depicts a low-pass circuit prototype of tri-coupled resonators, where L, R and C denote the inductance, resistance and capacitance, respectively. e_s represents the voltage source and i is the loop current flowing in each resonator, and L_{12}, L_{13} and L_{23} represent the mutual inductances between resonators 1 and 2, resonators 1 and 3 and resonators 2 and 3, respectively.

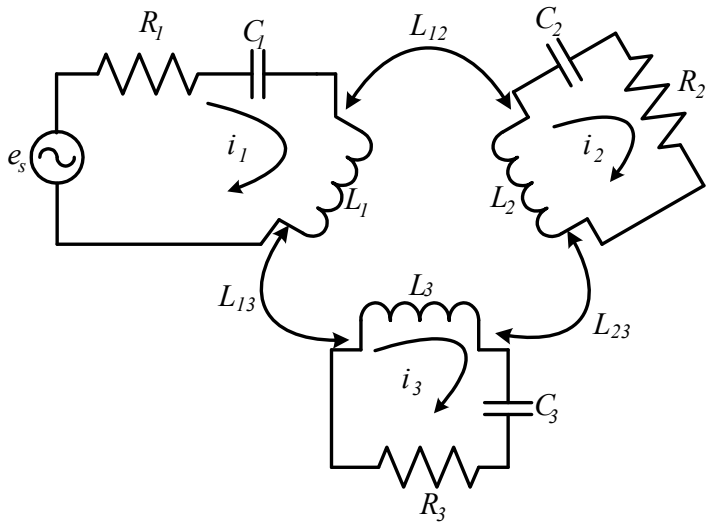

Figure 3.3 Equivalent circuit prototype of magnetically tri-coupled tri-resonator structure having three ports operating between source impedance R_1, representing port 1 and load impedances R_2 and R_3, representing ports 2 and 3 respectively.

The circuit is driven by a source of open-circuit voltage e_s with resistance R_1 and terminated by load impedances R_2 and R_3. Each loop is coupled to every other loop through mutual couplings and these couplings are assumed to be frequency-independent due to the narrow-band approximation [20].

To write the loop equations of the equivalent circuit shown in figure 3.3, Kirchhoff's voltage law (or Kirchhoff's loop rule) can be used. Kirchhoff's law states that the total

voltage around a closed loop must be zero. Therefore, the loop equations for figure 3.3 can be written as

$$\begin{aligned}
&\left(R_1 + j\omega L_1 + \frac{1}{j\omega C_1}\right) i_1 - j\omega L_{11} i_1 - j\omega L_{12} i_2 - j\omega L_{13} i_3 = e_s \\
&-j\omega L_{21} i_1 + \left(R_2 + j\omega L_2 + \frac{1}{j\omega C_2}\right) i_2 - j\omega L_{22} i_2 - j\omega L_{23} i_3 = 0 \\
&-j\omega L_{31} i_1 + \left(R_3 + j\omega L_3 + \frac{1}{j\omega C_3}\right) i_3 - j\omega L_{33} i_3 - j\omega L_{32} i_2 = 0
\end{aligned} \tag{3.4}$$

where $L_{ij} = L_{ji}$ represents the mutual inductance between resonators i and j where i=1, 2, 3 and j=1, 2, 3. A voltage-current relationship for each loop in equation (3.4) can be combined into the matrix form as

$$\begin{bmatrix} e_s \\ 0 \\ 0 \end{bmatrix} = \begin{bmatrix} R_1 + j\omega L_1 + \frac{1}{j\omega C_1} - j\omega L_{11} & -j\omega L_{12} & -j\omega L_{13} \\ -j\omega L_{21} & R_2 + j\omega L_2 + \frac{1}{j\omega C_2} - j\omega L_{22} & -j\omega L_{23} \\ -j\omega L_{31} & -j\omega L_{32} & R_3 + j\omega L_3 + \frac{1}{j\omega C_3} - j\omega L_{33} \end{bmatrix} \begin{bmatrix} i_1 \\ i_2 \\ i_3 \end{bmatrix} \tag{3.5}$$

Equation (3.5) can be expressed as

$$[e_s] = [Z] \cdot [i]$$

where $[Z]$ is a 3×3 impedance matrix.

Since all series resonators have the same resonant frequency, the filter of the equivalent circuit model in figure 3.3 is synchronously tuned. If all resonators are synchronously tuned, they would resonate at the same resonant frequency, ω_0 given by

$$\omega_0 = \frac{1}{\sqrt{LC}}$$

where $L = L_1 = L_2 = L_3$ and $C = C_1 = C_2 = C_3$

The impedance matrix in equation (3.5) can be expressed by

$$[Z] = L.\omega_0.FBW.[\overline{Z}] \tag{3.6}$$

where FBW is the fractional bandwidth of filter and given by $FBW = \Delta\omega/\omega_0$, and $[\overline{Z}]$ is the normalised impedance matrix shown as

$$[\overline{Z}] = \frac{[Z]}{L.\omega_0.FBW} \tag{3.7}$$

Equation (3.7) may be written in more expanded form as

$$[\overline{Z}] = \begin{bmatrix} \frac{[Z]_{11}}{L.\omega_0.FBW} & \frac{[Z]_{12}}{L.\omega_0.FBW} & \frac{[Z]_{13}}{L.\omega_0.FBW} \\ \frac{[Z]_{21}}{L.\omega_0.FBW} & \frac{[Z]_{22}}{L.\omega_0.FBW} & \frac{[Z]_{23}}{L.\omega_0.FBW} \\ \frac{[Z]_{31}}{L.\omega_0.FBW} & \frac{[Z]_{32}}{L.\omega_0.FBW} & \frac{[Z]_{33}}{L.\omega_0.FBW} \end{bmatrix}$$

$$\left[\overline{Z}\right]=\begin{bmatrix} \frac{R_1}{L.\omega_0.FBW}+p & \frac{-j\omega L_{12}}{L.\omega_0.FBW} & \frac{-j\omega L_{13}}{L.\omega_0.FBW} \\ \frac{-j\omega L_{21}}{L.\omega_0.FBW} & \frac{R_2}{L.\omega_0.FBW}+p & \frac{-j\omega L_{23}}{L.\omega_0.FBW} \\ \frac{-j\omega L_{31}}{L.\omega_0.FBW} & \frac{-j\omega L_{32}}{L.\omega_0.FBW} & \frac{R_3}{L.\omega_0.FBW}+p \end{bmatrix} \tag{3.8}$$

Defining p as a complex lowpass frequency variable, and given by

$$p=\frac{[Z]_{ii}-R_i}{L.\omega_0.FBW}, \text{ for } i=1,\ 2,\ 3$$

$$=\frac{j\omega L_1+\frac{1}{j\omega C_1}-j\omega L_{11}}{L.\omega_0.FBW}=\frac{j\omega L_1}{L.\omega_0.FBW}+\frac{L.\omega_0.FBW}{j\omega C_1}-\frac{j\omega L_{11}}{L.\omega_0.FBW}$$

$$\Rightarrow\ p=j\frac{1}{FBW}\left(\frac{\omega}{\omega_0}-\frac{\omega_0}{\omega}\right)$$

Defining the external quality factors, $Q_{ei}=\omega_0 L/R_{i=1,2,3}$ of the three resonators shown in Figure 3.3 for i=1, 2, 3 and the coupling coefficient, $M_{ij}=L_{ij}/L$ and assuming $\omega/\omega_0\approx 1$ for a narrow-band approximation, equation (3.8) can be simplified as

$$\left[\overline{Z}\right]=\begin{bmatrix} \frac{1}{q_{e1}}+p & -jm_{12} & -im_{13} \\ -jm_{21} & \frac{1}{q_{e2}}+p & -jm_{23} \\ -jm_{31} & -jm_{23} & \frac{1}{q_{e3}}+p \end{bmatrix} \tag{3.9}$$

Where q_{e1}, q_{e2} are q_{e3} are normalised external quality factors given by $q_{ei} = Q_{ei}.FBW$, for $i = 1,\ 2,3$ and m_{ij} is the normalised coupling coefficient and given by

$$m_{ij} = \frac{M_{ij}}{FBW} \tag{3.10}$$

For the case that the coupled resonators are asynchronously tuned, the circuit prototype in figure 3.3 can be modified by including the self couplings m_{11}, m_{22} and m_{33} as shown in figure 3.4.

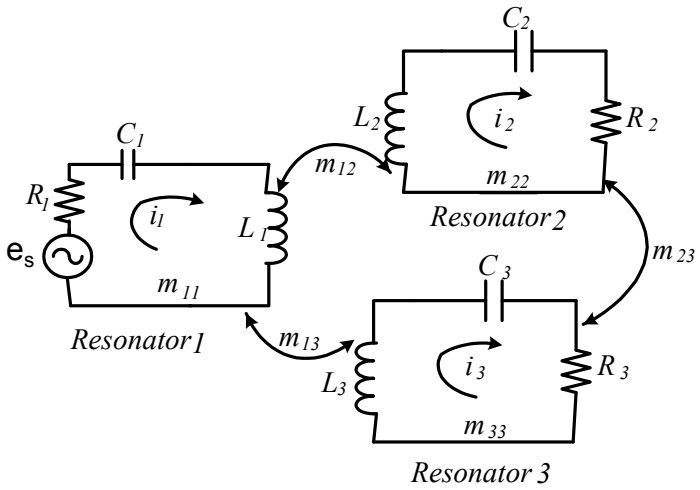

Figure 3.4 A circuit prototype for asynchronously tuned tri-coupled tri-resonator filter showing self couplings.

Thus, the normalised impedance matrix for the asynchronously tuned filters can be shown as

$$\left[\overline{Z}\right]=\begin{bmatrix} \frac{1}{q_{e1}}+p-jm_{11} & -jm_{12} & -jm_{13} \\ -jm_{21} & \frac{1}{q_{e2}}+p-jm_{22} & -jm_{23} \\ -jm_{31} & -jm_{23} & \frac{1}{q_{e3}}+p-jm_{33} \end{bmatrix} \tag{3.11}$$

Asynchronously tuned coupled resonators indicate that there is a self coupling between each resonator, represented by a non-zero coupling coefficient, m_{ii} for i in this case is 1, 2 and 3. The concept of coupling coefficient is further discussed in section 3.4 when we discuss inter-resonator coupling and cross-coupling of resonators.

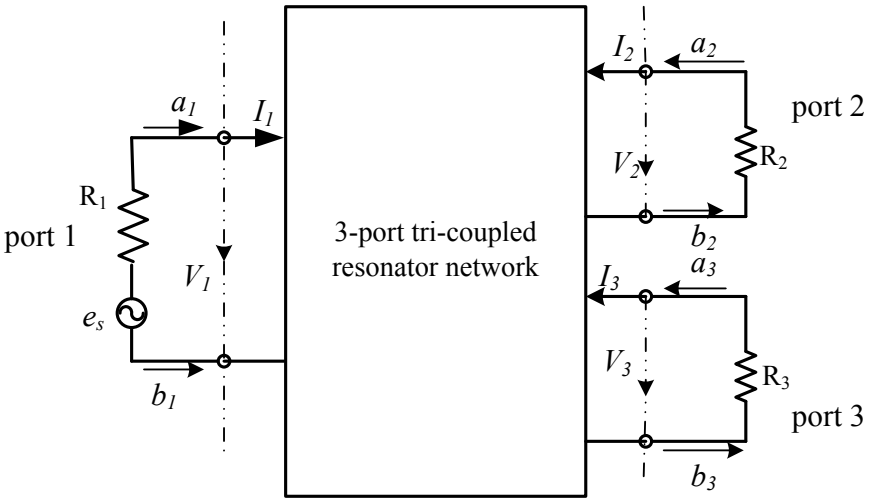

Figure 3.5 Network representation of an equivalent 3-port tri-coupled resonator circuit shown in figure 3.3, where a_1, a_2, a_3 and b_1, b_2, b_3 are wave variables representing incident and reflected waves, respectively.

Now consider the wave variables shown in figure (3.5). From the transmission line theory, the incident and reflected waves are related by [9]

$$b_i = \sum_j^n S_{ij} a_j \text{ for } i = 1,\ 2,\ 3,....n \tag{3.12}$$

where

$S_{ij} = \Gamma_{ij}$, is the reflection coefficient of the ith port if $i = j$ with all other ports matched

$S_{ij} = T_{ij}$, is the forward transmisson coefficient of the jth port if $i > j$ with all other ports matched

$S_{ij} = T_{ij}$, is the reverse transmission coefficient of the jth port if $i < j$ with all all other ports matched

In general, for n=3, equation (3.12) can be written as

$$\begin{aligned} b_1 &= S_{11}a_1 + S_{12}a_2 + S_{13}a_3 \\ b_2 &= S_{21}a_1 + S_{22}a_2 + S_{23}a_3 \\ b_3 &= S_{31}a_3 + S_{32}a_2 + S_{33}a_3 \end{aligned} \tag{3.13}$$

Equation (3.13) may be described in matrix form as

$$\begin{bmatrix} b_1 \\ b_2 \\ b_3 \end{bmatrix} = \begin{bmatrix} S_{11} & S_{12} & S_{13} \\ S_{21} & S_{22} & S_{23} \\ S_{31} & S_{32} & S_{33} \end{bmatrix} \begin{bmatrix} a_1 \\ a_2 \\ a_3 \end{bmatrix} \tag{3.14}$$

The relationship between $a,\ b,\ V$ and I are given by [9]

$$a_n = \frac{1}{2}\left(\frac{V_i}{\sqrt{R_i}} + \sqrt{R_i} I_i\right), \quad b_n = \frac{1}{2}\left(\frac{V_i}{\sqrt{R_i}} - \sqrt{R_i} I_i\right) \text{ for } i=1,2,\ldots n \tag{3.15}$$

From the circuit of figures 3.3 and its network representation in figure 3.5, it can be identified that $V_1 = e_s - i_1 R_1$ and $I_1 = i_1,\ I_2 = -i_2,\ I_3 = -i_3$, where in this case $i_1,\ i_2$ and i_3 are loop currents, and using them in equation (3.15) yields

$$\begin{aligned}
a_1 &= \frac{1}{2}\left(\frac{V_1}{\sqrt{R_1}} + \sqrt{R_1} i_1\right) = \frac{1}{2}\left(\frac{e_s - i_1 R_1}{\sqrt{R_1}} + \sqrt{R_1} i_1\right) = \frac{1}{2}\frac{e_s}{\sqrt{R_1}} \\
a_2 &= \frac{1}{2}\left(\frac{V_2}{\sqrt{R_2}} + \sqrt{R_2} i_2\right) = \frac{1}{2}\left(\frac{-i_2 R_2}{\sqrt{R_2}} + \sqrt{R_2} i_2\right) = 0 \\
a_3 &= \frac{1}{2}\left(\frac{V_3}{\sqrt{R_2}} + \sqrt{R_3} i_3\right) = \frac{1}{2}\left(\frac{-i_3 R_3}{\sqrt{R_2}} + \sqrt{R_3} i_3\right) = 0
\end{aligned} \tag{3.16}$$

$$\begin{aligned}
b_1 &= \frac{1}{2}\left(\frac{V_1}{\sqrt{R_1}} - \sqrt{R_1} i_1\right) = \frac{1}{2}\left(\frac{e_s - i_1 R_1}{\sqrt{R_1}} - \sqrt{R_1} i_1\right) = \frac{e_s - 2 i_1 R_1}{2\sqrt{R_1}} \\
b_2 &= \frac{1}{2}\left(\frac{V_2}{\sqrt{R_2}} - \sqrt{R_2} i_2\right) = \frac{1}{2}\left(\frac{-(-i_2 R)_2}{\sqrt{R_2}} - \sqrt{R_2}(-i_2)\right) = \frac{1}{2}\left(\frac{i_2 R_2 + R_2 i_2}{\sqrt{R_2}}\right) = i_2\sqrt{R_2} \\
b_3 &= \frac{1}{2}\left(\frac{V_3}{\sqrt{R_2}} - \sqrt{R_3} i_3\right) = \frac{1}{2}\left(\frac{-(-i_3 R_3)}{\sqrt{R_2}} - (-i_3)\sqrt{R_3}\right) = \frac{1}{2}\left(\frac{i_3 R_3 + R_3 i_3}{\sqrt{R_3}}\right) = i_3\sqrt{R_3}
\end{aligned} \tag{3.17}$$

Substituting equations (3.16) and (3.17) into equation (3.14) yields

$$\begin{bmatrix} \frac{e_s - 2i_1R_1}{2\sqrt{R_1}} \\ i_2\sqrt{R_2} \\ i_3\sqrt{R_3} \\ \end{bmatrix} = \begin{bmatrix} S_{11} & S_{12} & S_{13} \\ S_{21} & S_{22} & S_{23} \\ S_{31} & S_{32} & S_{33} \end{bmatrix} \begin{bmatrix} \frac{1}{2}\frac{e_s}{\sqrt{R_1}} \\ 0 \\ 0 \\ \end{bmatrix} \tag{3.18}$$

From equation (3.18), the Scattering parameters S_{11}, S_{21} and S_{31} for a three port network can be evaluated at $a_2 = a_3 = 0$ as

$$\begin{aligned} S_{11} &= \frac{b_1}{a_1}\Big|_{a_2=a_3=0} = \frac{e_s - 2i_1R_1}{e_s} = 1 - \frac{2i_1R_1}{e_s} \\ S_{21} &= \frac{b_2}{a_1}\Big|_{a_2=a_3=0} = \frac{2i_2\sqrt{R_1R_2}}{e_s} \\ S_{31} &= \frac{b_3}{a_1}\Big|_{a_2=a_3=0} = S_{31} = \frac{2i_3\sqrt{R_1R_3}}{e_s} \end{aligned} \tag{3.19}$$

From equation (3.6) and (3.7), the loop current i is worked out as

$$\begin{aligned} [i] &= \frac{[e_s]}{L.\omega_0.FBW.\left[\overline{Z}\right]_{ij}} = \frac{[e_s]}{L.\omega_0.FBW}\left[\overline{Z}\right]_{ij}^{-1} \\ \rightarrow i_1 &= \frac{e_s}{L.\omega_0.FBW}\left[\overline{Z}\right]_{11}^{-1}, \rightarrow i_2 = \frac{e_s}{L.\omega_0.FBW}\left[\overline{Z}\right]_{21}^{-1}, \rightarrow i_3 = \frac{e_s}{L.\omega_0.FBW}\left[\overline{Z}\right]_{31}^{-1} \end{aligned} \tag{3.20}$$

Making use of $Q_{ei} = \omega_0 L / R_{i=1,2,3}$, $q_{ei} = \left(Q_{ei}.FBW\right)$ and equation (3.20) into (3.19) we get

$$\begin{aligned} S_{11} &= 1 - \frac{2}{q_{e1}}\left[\overline{Z}\right]^{-1}_{11} \\ S_{21} &= 2\frac{1}{\sqrt{q_{e1}q_{e2}}}\left[\overline{Z}\right]^{-1}_{21} \\ S_{31} &= 2\frac{1}{\sqrt{q_{e1}q_{e3}}}\left[\overline{Z}\right]^{-1}_{31} \end{aligned} \tag{3.21}$$

3.3.2. Electric Coupling

This section describes the derivation of 3×3 coupling matrix of electrically coupled tri-resonator structure with three ports, where in this case the electric coupling is represented by capacitor. In a similar way to the normalised impedance matrix $\left[\overline{Z}\right]$ obtained in section 3.3.1 above, the normalised admittance matrix $\left[\overline{Y}\right]$ will be derived in this section. Electrically tri-coupled tri-resonator circuit is shown in figure 3.6, where v_i for i =1, 2 and 3 denotes the node voltage, G_i for i =1, 2 and 3 represents ports conductance, i_s is the source current and C_{12}, C_{13} and C_{23} represent the mutual capacitances across resonators 1 and 2, resonators 1 and 3 and resonators 2 and 3, respectively. Energy may be coupled between adjacent resonators by electric coupling. To compute the node equations, Kirchhoff's current law is applied to the equivalent circuit prototype of tri-resonator circuit shown in Figure 3.6. This law states that the algebraic sum of currents leaving a node in a network is zero. The node voltage equations are formulated as

$$\begin{aligned}
&\left(G_1 + j\omega C_1 + \frac{1}{j\omega L_1}\right)v_1 - j\omega C_{11}v_1 - j\omega C_{12}v_2 - j\omega C_{13}v_3 = i_s \\
&-j\omega C_{21}v_1 + \left(G_2 + j\omega C_2 + \frac{1}{j\omega L_2}\right)v_2 - j\omega C_{22}v_2 - j\omega C_{23}v_3 = 0 \\
&-j\omega C_{31}v_1 + \left(G_3 + j\omega C_3 + \frac{1}{j\omega L_3}\right)v_3 - j\omega C_{33}v_3 - j\omega C_{32}v_2 = 0
\end{aligned} \tag{3.22}$$

Equation (3.22) can be expressed in matrix form as

$$\begin{bmatrix} i_s \\ 0 \\ 0 \end{bmatrix} = \begin{bmatrix} G_1 + j\omega C_1 + \frac{1}{j\omega L_1} - j\omega C_{11} & -j\omega C_{12} & -j\omega C_{13} \\ -j\omega C_{21} & G_2 + j\omega C_2 + \frac{1}{j\omega L_2} - j\omega C_{22} & -j\omega C_{23} \\ -j\omega C_{31} & -j\omega C_{32} & G_3 + j\omega C_3 + \frac{1}{j\omega L_3} - j\omega C_{33} \end{bmatrix} \begin{bmatrix} v_1 \\ v_2 \\ v_3 \end{bmatrix} \tag{3.23}$$

or equivalently $[i] = [Y].[v]$, where $[Y]$ is admittance matrix.

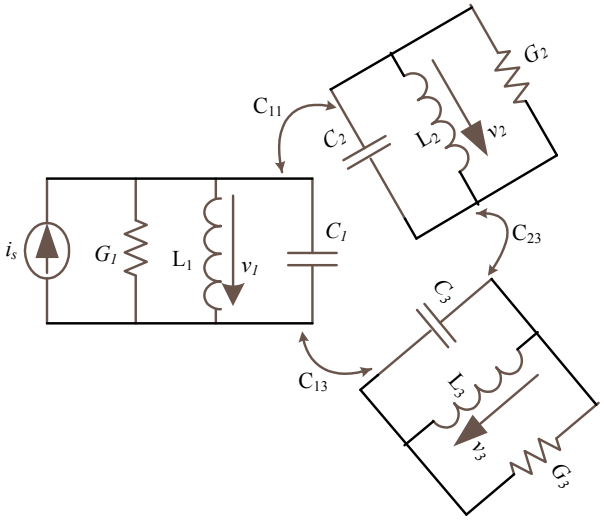

Figure 3.6 Equivalent circuit prototype of electrically coupled tri-resonator having three ports operating between source conductance G_1 and load conductance G_2 and G_3

If all resonators are synchronously tuned at the same resonant frequency of $\omega_0 = \left(\sqrt{LC}\right)^{-1}$, where $L = L_1 = L_2 = L_3$ and C=$C_1 = C_2 = C_3$, the admittance matrix $[Y]$ can be expressed by

$$[Y] = C.\omega_0.FBW\left[\overline{Y}\right] \tag{3.24}$$

where *FBW* is the fractional bandwidth, and $\left[\overline{Y}\right]$ is the normalised admittance matrix.

From equation (3.24), the admittance matrix can be expressed as

$$\left[\overline{Y}\right] = \frac{[Y]}{C.\omega_0.FBW} = \begin{bmatrix} \frac{[Y]_{11}}{C.\omega_0.FBW} & \frac{[Y]_{12}}{C.\omega_0.FBW} & \frac{[Y]_{13}}{C.\omega_0.FBW} \\ \frac{[Y]_{21}}{C.\omega_0.FBW} & \frac{[Y]_{22}}{C.\omega_0.FBW} & \frac{[Y]_{23}}{C.\omega_0.FBW} \\ \frac{[Y]_{31}}{C.\omega_0.FBW} & \frac{[Y]_{32}}{C.\omega_0.FBW} & \frac{[y]_{33}}{C.\omega_0.FBW} \end{bmatrix}$$

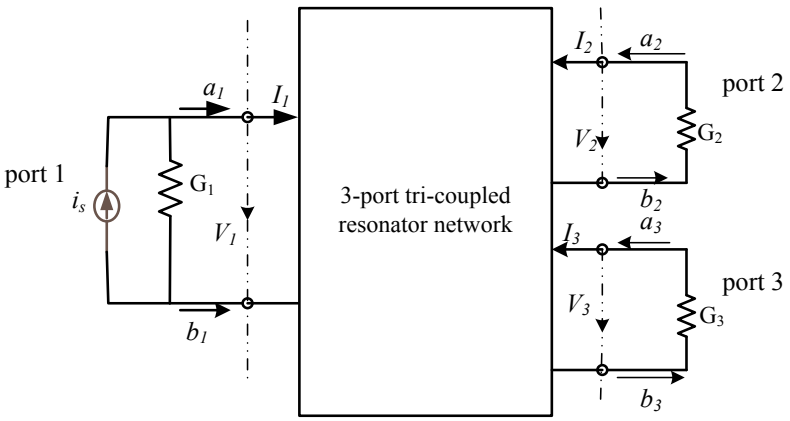

Figure 3.7 Network representation of 3-port tri-coupled resonator in figure 3.6 where a_1, a_2, a_3 and b_1, b_2, b_3 are wave variables representing incident and reflected waves, respectively.

$$\left[\overline{Y}\right]=\begin{bmatrix} \dfrac{G_1}{C.\omega_0.FBW}+p & \dfrac{-j\omega C_{12}}{C.\omega_0.FBW} & \dfrac{-j\omega C_{13}}{C.\omega_0.FBW} \\ \dfrac{-j\omega C_{21}}{C.\omega_0.FBW} & \dfrac{G_2}{C.\omega_0.FBW}+p & \dfrac{-j\omega C_{23}}{C.\omega_0.FBW} \\ \dfrac{-j\omega C_{31}}{C.\omega_0.FBW} & \dfrac{-j\omega C_{32}}{C.\omega_0.FBW} & \dfrac{G_3}{C.\omega_0.FBW}+p \end{bmatrix} \tag{3.25}$$

where p is the complex lowpass frequency variable as defined in the previous section.

Defining the external quality factors, $Q_{ei}=\omega_0 C/G_{i=1,2,3}$ of the three resonators shown in figure 3.6 for i=1, 2, 3 and the coupling coefficient, $M_{ij}=C_{ij}/C$ and assuming $\omega/\omega_0 \approx 1$ for a narrow-band approximation, equation (3.25) can be simplified as

$$\left[\overline{Y}\right]=\begin{bmatrix} \dfrac{1}{q_{e1}}+p & -jm_{12} & -jm_{13} \\ -jm_{21} & \dfrac{1}{q_{e2}}+p & -jm_{23} \\ -jm_{31} & -jm_{23} & \dfrac{1}{q_{e3}}+p \end{bmatrix} \tag{3.26}$$

Where q_{e1}, q_{e2} are q_{e3} are normalised external quality factors given by $q_{ei}=Q_{ei}.FBW$, for i=1, 2, 3 and m_{ij} is the normalised coupling coefficient given in equation (3.10).

For asynchronously tuning, where all resonators may resonate at different frequency, normalised admittance matrix, $\left[\overline{Y}\right]$ contains an additional entries m_{11}, m_{22} and m_{33} on the main diagonal, which accounts for self coupling of each resonator to itself, and is

analogous to the normalised impedance of asynchronously tuned resonators shown in equation (3.11), and given by

$$\left[\overline{Y}\right]=\begin{bmatrix} \frac{1}{q_{e1}}+p-jm_{11} & -jm_{12} & -im_{13} \\ -jm_{21} & \frac{1}{q_{e2}}+p-jm_{22} & -jm_{23} \\ -jm_{31} & -jm_{23} & \frac{1}{q_{e3}}+p-jm_{33} \end{bmatrix} \tag{3.27}$$

To derive the three-port S-parameters of a tri-coupled resonator, the wave variables in the three-port network representation in figure 3.7 are related to voltage and current variables, V_n and I_n as in equation (3.28). The relationship between a, b, V and I in figure 3.6 can be derived from equation (3.14) by replacing $1/G_n$ for R_n, and expressed as

$$\begin{aligned} a_n &= \frac{1}{2}\left(V_n\sqrt{G_n}+\frac{I_n}{\sqrt{G_n}}\right) \\ b_n &= \frac{1}{2}\left(V_n\sqrt{G_n}-\frac{I_n}{\sqrt{G_n}}\right) \end{aligned} \quad \text{for } n=1,2,3 \tag{3.28}$$

By inspecting the circuit of figure 3.6, and its network representation in figure 3.7, one can identify that $V_1=v_1$, $V_2=v_2$, $V_3=v_3$ and $I_1=i_s-v_1G_1$, where v_1, v_2 and v_3 are node voltages at resonators 1, 2 and 3, respectively, and thus equation (3.28) can be simplified to

$$a_1 = \frac{1}{2}\left(V_1\sqrt{G_1} + \frac{I_1}{\sqrt{G_1}} \right) = \frac{1}{2}\left(V_1\sqrt{G_1} + \frac{i_s - v_1 G_1}{\sqrt{G_1}} \right) = \frac{1}{2}\left(\frac{e_s - v_1 G_1 + G_1 v_1}{\sqrt{G_1}} \right)$$

$$\rightarrow a_1 = \frac{1}{2}\frac{i_s}{\sqrt{G_1}}, \rightarrow a_2 = 0, \rightarrow a_3 = 0 \tag{3.29}$$

Similarly from

$$b_n = \frac{1}{2}\left(V_n\sqrt{G_n} - \frac{I_n}{\sqrt{G_n}} \right),$$

we obtain the reflected wave variables b_1, b_2 and b_3 as shown in equation (3.30)

$$\rightarrow b_1 = \frac{2v_1 G_1 - i_s}{2\sqrt{G_1}}, \quad \rightarrow b_2 = v_2\sqrt{G_2}, \quad \rightarrow b_3 = v_3\sqrt{G_3} \tag{3.30}$$

Substituting equations (3.29) and (3.30) into equation (3.18) yields

$$\begin{bmatrix} \frac{2v_1 G_1 - i_s}{2\sqrt{G_1}} \\ v_2\sqrt{G_2} \\ v_3\sqrt{G_3} \\ \end{bmatrix} = \begin{bmatrix} S_{11} & S_{12} & S_{13} \\ S_{21} & S_{22} & S_{23} \\ S_{31} & S_{32} & S_{33} \end{bmatrix} \begin{bmatrix} \frac{1}{2}\frac{i_s}{\sqrt{G_1}} \\ 0 \\ 0 \\ \end{bmatrix} \tag{3.31}$$

From equation (3.31) the S-parameters can be derived as

$$
\begin{aligned}
S_{11} &= \frac{b_1}{a_1}\Big|_{a_2=a_3=0} = \frac{2v_1G_1 - i_s}{i_s}, \;\rightarrow\; S_{11} = \frac{2v_1G_1}{i_s} - 1 \\
S_{21} &= \frac{b_2}{a_1}\Big|_{a_2=a_3=0} = \frac{2v_2\sqrt{G_1G_2}}{i_s} \\
S_{31} &= \frac{b_3}{a_1}\Big|_{a_2=a_3=0} = \frac{2v_3\sqrt{G_1G_3}}{i_s}
\end{aligned}
\tag{3.32}
$$

By combining equations (3.23) and (3.24), the node voltage v can be obtained as

$$
\begin{aligned}
[v] &= \frac{[i_s]}{C.\omega_0.FBW.\left[\overline{Y}\right]_{ij}} = \frac{[i_s]}{C.\omega_0.FBW}\left[\overline{Y}\right]_{ij}^{-1} \\
\rightarrow v_1 &= \frac{i_s}{C.\omega_0.FBW}\left[\overline{Y}\right]_{11}^{-1}, \rightarrow v_2 = \frac{i_s}{C.\omega_0.FBW}\left[\overline{Y}\right]_{21}^{-1}, \rightarrow v_3 = \frac{i_s}{C.\omega_0.FBW}\left[\overline{Y}\right]_{31}^{-1}
\end{aligned}
\tag{3.33}
$$

Substitution of equation (3.33) into (3.32), and making use of $Q_{ei} = \omega_0 C/G_i$ and $q_{ei} = \left(Q_{ei}.FBW\right)$ for $i = 1,\ 2$ and 3 into (3.32) yields

$$
\begin{aligned}
S_{11} &= 1 - \frac{2}{q_{e1}}\left[\overline{Y}\right]_{11}^{-1} \\
S_{21} &= 2\frac{1}{\sqrt{q_{e1}q_2}}\left[\overline{Y}\right]_{21}^{-1} \\
S_{31} &= 2\frac{1}{\sqrt{q_{e1}q_3}}\left[\overline{Y}\right]_{31}^{-1}
\end{aligned}
\tag{3.34}
$$

From the derivations in previous and this section, for magnetic and electric coupling of a general 3×3 coupling matrix of magnetically and electrically coupled tri-resonator

structure for three-port network, the normalised impedance matrix for magnetically coupled and admittance matrix of electrically coupled resonators are identical. Therefore, the S-parameters of a three-port network of a tri-coupled tri-resonator structure in equations (3.21) and (3.34) can be incorporated into one form as

$$\begin{aligned} S_{11} &= 1 - \frac{2}{q_{e1}}\left[\overline{A}\right]^{-1}_{11} \\ S_{21} &= 2\frac{1}{\sqrt{q_{e1}q_{e2}}}\left[\overline{A}\right]^{-1}_{21} \\ S_{31} &= 2\frac{1}{\sqrt{q_{e1}q_{e3}}}\left[\overline{A}\right]^{-1}_{31} \end{aligned} \tag{3.35}$$

with $[\mathrm{A}] = [q] + p[U] - j[m]$, where $[U]$ is a 3×3 identity matrix, $[q]$ is a 3×3 matrix with all entries zero except for $q_{11} = \frac{1}{q_{e1}}, q_{22} = \frac{1}{q_{e2}}$ and $q_{33} = \frac{1}{q_{e3}}$, $[m]$ is the general 3×3 normalised coupling matrix [1].

The extension of the general S-parameters shown in equation (3.35) for the synthesis of a three-port coupled resonator power splitter is discussed in the next subsequent chapters in detail.

The thesis realises the proposed tri-coupled resonator structures by developing mathematical relations to calculate the normalised coupling coefficients, m and external quality factor, q_e at the input and output ports. This is one of the principal aims of this work. From S-parameters of a three-port network in equation (3.35), a mathematical

analysis is extended to derive general equations to compute coupling parameters so that a power splitter is analysed and designed.

3.4. Direct and Cross Coupling

To demonstrate the concept of direct coupling between adjacent resonators and the cross coupling between nonadjacent resonators, the bandpass circuit prototype shown in figure 3.8 is used.

The normalised coupling matrix, $[m]$ for a tri-resonator filter is a 3×3 symmetric matrix, i.e., $m = m^T$, or $m_{ij} = m_{ji}$ where the normalised coupling coefficients, m_{ij} represent the values of couplings between the resonators of the bandpass filter. The coupling coefficients are the ratio of the coupled to the stored electromagnetic energies and may take either a positive or negative sign. A negative sign indicates that the coupling decreases the stored energy of the uncoupled resonators and a positive sign indicates that it increases [1]. For a normalised coupling matrix m, which is a 3×3 symmetric coupling matrix is given by

$$[m] = \begin{bmatrix} 0 & m_{12} & m_{13} \\ m_{21} & 0 & m_{23} \\ m_{31} & m_{23} & 0 \end{bmatrix}$$

In the case of synchronously tuned resonators (and symmetric frequency responses), the values of the coupling coefficients on the main diagonal (m_{ii}) are always zero. The sub-

diagonal entries (m_{12} and m_{23}) are direct (or sequential) couplings between adjacent resonators.

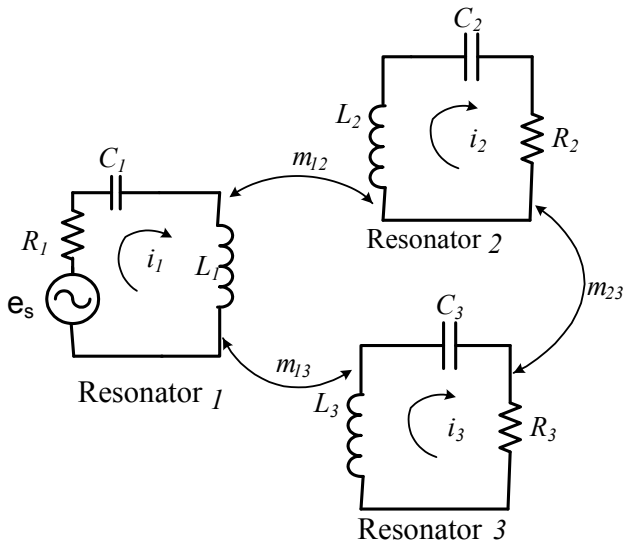

Figure 3.8 A bandpass circuit prototype for a tri-coupled tri-resonator filter.

The couplings between all non-sequentially numbered resonators are said to be cross-couplings. The purpose of cross-coupling in filter design is for the reduction of the coupling matrix so as to minimise the number of resonators to be coupled. For a bandpass filter of the kind in figure 3.7, the cross coupling would occur only between resonators 1 and 3, and represented by m_{13}.

As mentioned in previous section, asymmetric filter frequency response (or asynchronously tuned filter) has non-zero entries on the main diagonal of the normalised coupling matrix, $[m]$, and are self coupling. The self coupling account for differences in the resonant frequencies of the different resonators. A 3×3 asymmetric coupling matrix is given as

$$[m] = \begin{bmatrix} m_{11} & m_{12} & m_{13} \\ m_{21} & m_{22} & m_{23} \\ m_{31} & m_{23} & m_{33} \end{bmatrix}$$

where m_{11}, m_{22} and m_{33} are self-coupling coefficients.

Chapter 4

Passive Microwave Circuits

4.1. Introduction

Microwave circuits are composed of distributed elements with dimensions such that the voltage and phase over the length of the device can vary significantly [3]. They can also be lumped elements. By modifying the lengths and dimensions of the device, the line voltage, current amplitude and phase can be effectively controlled in such away to obtain a specifically desired frequency response of the device [3].

A microwave filter is a two-port microwave circuit whose frequency response provides transmission at desired frequencies and attenuation at other frequencies. An ideal filter should perform this function without adding or generating new frequency components, while at the same time having a linear phase response.

The microwave filter is a vital component in a huge variety of electronic systems; including mobile radio, satellite communications and radar. They find their use in excess of applications in areas of wireless communications, wireless networking, digital communications, target detection and identification, imaging, deep space communications, medical imaging and treatment, and radio spectrometry [28].

Such components are used to select or reject signals at different frequencies. Although the physical realisation of microwave filters may vary, the circuit network theory is common to all.

In the next section passive microwave circuits such as power splitters will be presented, and a practical filter design using coupling matrix synthesis is demonstrated. It is also shown that coupling matrix synthesis may be used to have a better understanding and examine the various calculated filter responses.

4.2. Passive Filters

Passive filters, often consisting of only two or three components are used to reduce (attenuate) the amplitude of signals. They are frequency selective, so they can reduce the signal amplitude at some frequencies without affecting others. To indicate the effect a filter has on wave amplitude at different frequencies, a frequency response graph is shown in Figure 4.1. This graph plots the loss (on the vertical axis) against the frequency of a passive filter, and shows the relative output levels over a band of different frequencies.

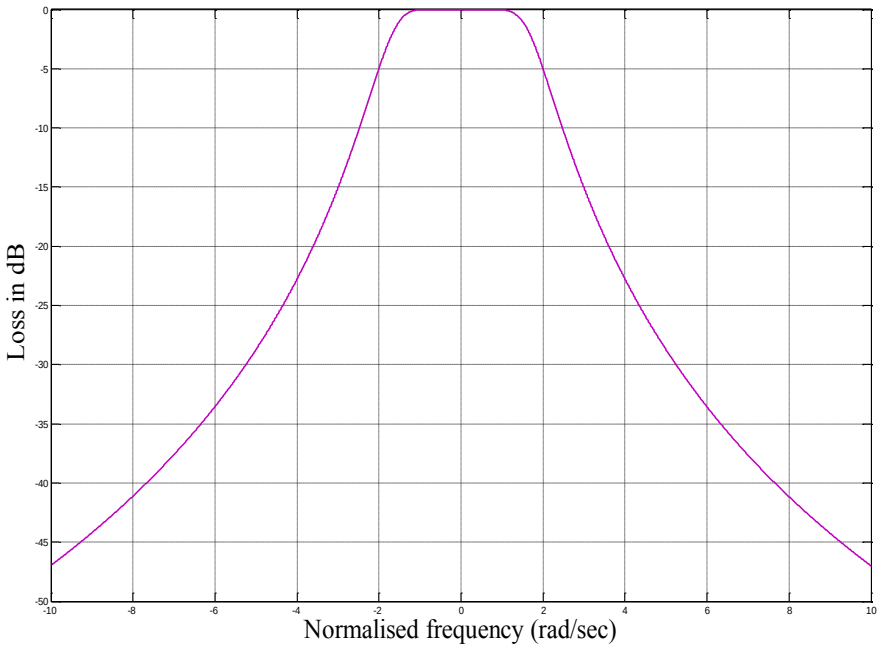

Figure 4.1 Passive filter responses

Passive filters only contain components such as capacitors and inductors. This means that, the signal amplitude at a filter output cannot be larger than the input. Passive filters do not require any external power supply and are adequately used in many applications.

4.2.1. Power Splitters

Power splitters are passive circuits with a paramount importance in signal splitting and combining. As mentioned in previous section, they are widely used in base stations, antenna arrays, and generally in building wireless communication systems and signal processing applications.

Besides splitting power, they also can act as power combiners because they are bi-directional/reciprocal devices. That is, they can be used to combine power from output ports into an input port. To investigate if an ideal power divider would be matched at all ports, lossless and reciprocal, three port microwave network representation in figure 4.1 is used.

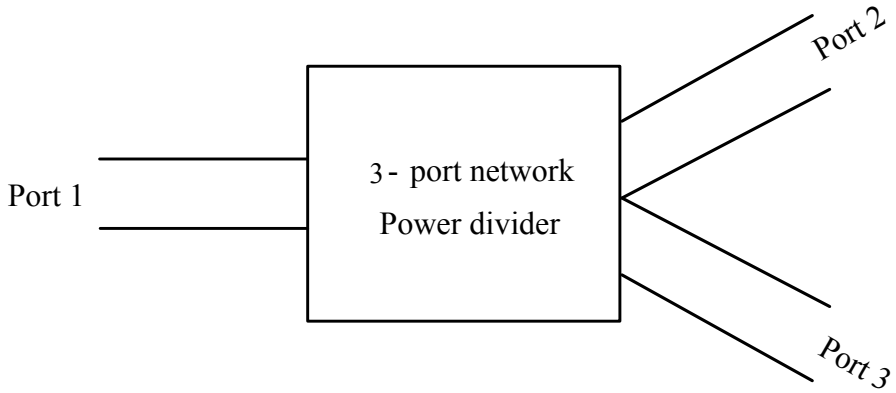

Figure 4.2 A three-port network representation used as a power divider.

The scattering (S) matrix for a 3-port microwave network is given by

$$[S]=\begin{bmatrix} S_{11} & S_{12} & S_{13} \\ S_{21} & S_{22} & S_{23} \\ S_{31} & S_{32} & S_{33} \end{bmatrix} \tag{4.1}$$

Assuming all the three- ports are matched so that $S_{ii}=0$, this implies $S_{11}=S_{22}=S_{33}=0$, and that the network is reciprocal so that $S_{ij}=S_{ji}$, that is for a 3×3 S-matrix, $S_{12}=S_{21}$, $S_{13}=S_{31}$ and $S_{23}=S_{32}$. With these properties, the general S-matrix for a device is

$$[S]=\begin{bmatrix} 0 & S_{12} & S_{13} \\ S_{21} & 0 & S_{23} \\ S_{31} & S_{32} & 0 \end{bmatrix} \tag{4.2}$$

For a lossless junction the scattering matrix is a unitary matrix [3]. This means that the sum of the product of the elements in any row with the complex conjugate of the elements in any other row is zero. Condition of unitary and principle of conservation of energy leads to equation (4.3)

$$\begin{aligned} |S_{12}|^2+|S_{13}|^2&=1 \qquad & S_{13}S_{23}^*&=0 \\ |S_{12}|^2+|S_{23}|^2&=1 \qquad & S_{12}S_{13}^*&=0 \\ |S_{13}|^2+|S_{23}|^2&=1 \qquad & S_{12}S_{23}^*&=0 \end{aligned} \tag{4.3}$$

Equation (4.3) can be satisfied in the following way

$$S_{12} = S_{23} = S_{31} = 0 \qquad |S_{12}| = |S_{32}| = |S_{13}| = 1$$

or (4.4)

$$S_{21} = S_{32} = S_{13} = 0 \qquad |S_{12}| = |S_{23}| = |S_{31}| = 1$$

Equation (4.4) implies that $S_{ij} \neq S_{ji}$ for $i \neq j$. Under this condition, the device must be non reciprocal. The second column of equation (4.3) shows that at least two of the three unique S-parameters must be zero. But if two of them were zero, then one of the equations in the first column would be violated. From this we can conclude that it is impossible to have a lossless, matched and reciprocal three port device.

4.2.1.1. Insertion and Reflection Losses

For a 3-port power splitter with tri-coupled resonators, the insertion loss parameters between ports may be given by [8]

$$L_{A12} = -20\log|S_{21}|\,dB$$
$$L_{A13} = -20\log|S_{31}|\,dB \tag{4.5}$$

Where L_{A12} corresponds to the insertion loss between ports 1 and 2, and L_{A13} corresponds to the insertion loss between ports 1 and 3 of figure 4.1. Similarly, the reflection loss at port 1 may be defined as in [1] and [8]

$$L_R = -20\log|S_{11}|\,dB = -10\log|S_{11}|^2\,dB \tag{4.6}$$

The reflection loss is a measure of how well matched the network is. This is because it is a measure of reflected signal attenuation.

Applying conservation of energy formula to figure 4.3, we have

$$|S_{11}|^2 + |S_{21}|^2 + |S_{31}|^2 = 1 \tag{4.7}$$

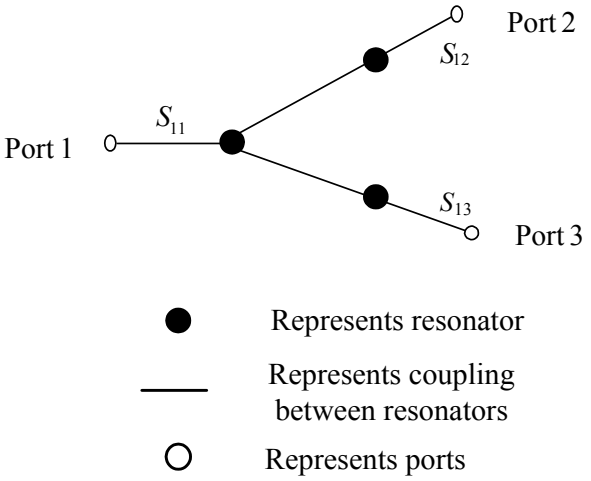

Figure 4.3: Tri-resonator power splitter prototype

Assume that the power at the input port is divided between the two output ports 2 and 3 such that

$$|S_{21}|^2 = \beta |S_{31}|^2, \ \beta < 1 \tag{4.8}$$

where β is a constant.

Now substituting equation (4.8) into (4.7), we have

$$|S_{11}|^2 = 1 - |S_{31}|^2 (\beta + 1) \tag{4.9}$$

Now making use of equation (4.9) into equation (4.6) yields

$$L_R = -10 \log\left(1 - |S_{31}|^2 (\beta + 1)\right) \tag{4.10}$$

Making $|S_{31}|$ a subject gives

$$|S_{31}| = \sqrt{\left(\frac{1}{\beta+1}\left(1-10^{-L_R/10}\right)\right)} \tag{4.11}$$

and similarly, the transmission coefficient, $|S_{21}|$ can be computed by substituting equation (4.11) into equation (4.8), and this yields

$$|S_{21}| = \sqrt{\left(\frac{\beta\left(1-10^{-L_R/10}\right)}{\beta+1}\right)} \tag{4.12}$$

To obtain the insertion loss between input and output ports, equations (4.11) and (4.12) can be used in (4.5) to yield

$$\begin{aligned} L_{A12} &= -20\log\left(\frac{\beta\left(1-10^{-L_R/10}\right)}{\beta+1}\right)^{\frac{1}{2}} dB = -10\log\left(\frac{\beta}{\beta+1}\right) dB - 10\log\left(1-10^{-L_R/10}\right) dB \\ L_{A13} &= -20\log\left(\frac{\left(1-10^{-L_R/10}\right)}{\beta+1}\right)^{\frac{1}{2}} dB = -10\log\left(\frac{1}{\beta+1}\right) dB - 10\log\left(1-10^{-L_R/10}\right) dB \end{aligned} \tag{4.13}$$

And it follows that the insertion loss and return loss are related as in equation (4.13), where the terms $10\log\left(\frac{\beta}{\beta+1}\right) dB$ and $10\log\left(\frac{1}{\beta+1}\right) dB$ correspond to the maximum values of $-|S_{21}|_{dB}$ and $-|S_{31}|_{dB}$, respectively [8].

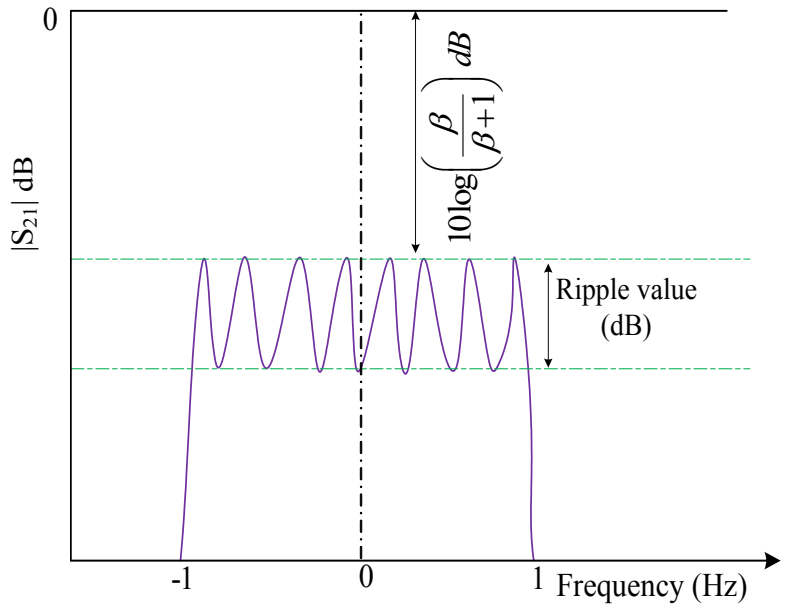

(a)

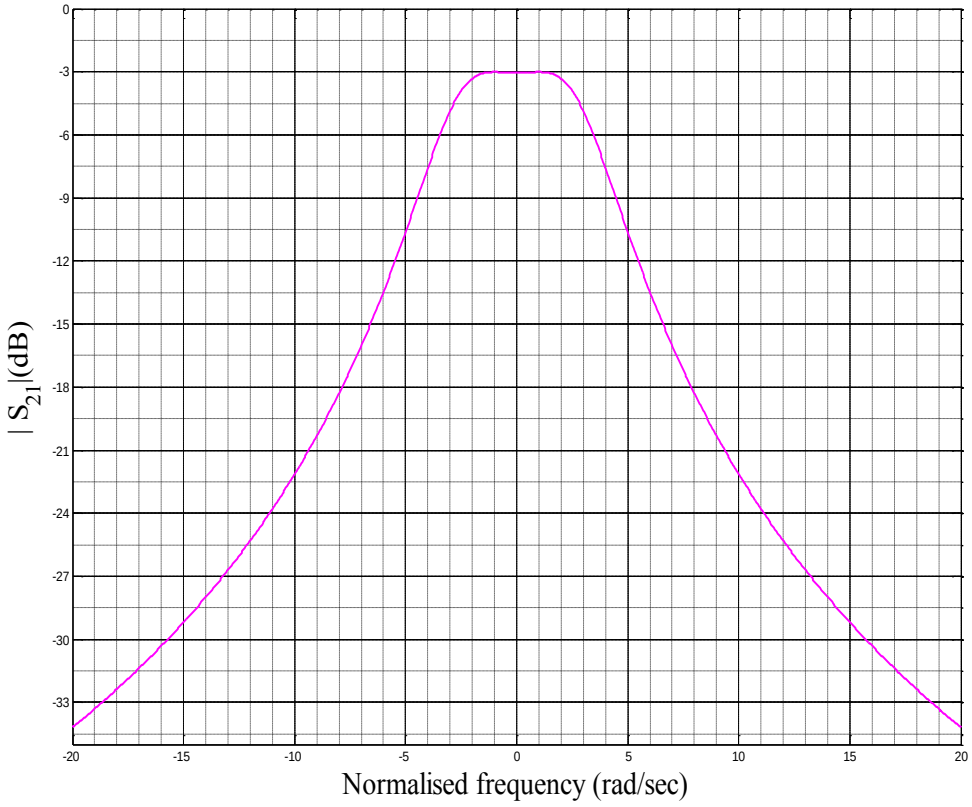

(b)

Figure 4.4: (a) Insertion Loss, S_{21} (dB) [8] and (b) 3-dB power splitter

4.2.1.2. Power Splitter Polynomial

In the case of a two-port lossless filter network composed of series of *N*-inter-coupled resonator filters, its reflection and transmission functions may be defined as a ratio of two N^{th} degree polynomials [30]

$$S_{11}(s) = \frac{F_N(s)}{E_N(s)} \qquad S_{21}(s) = \frac{P_N(s)}{\varepsilon E_N(s)} \tag{4.14}$$

where F, P and E are characteristic polynomials, and $s = j\omega$ is the complex frequency variable, and for Chebyshev filtering function, ε is a normalising constant for the transmission coefficient to the equiripple level at $\omega = \pm 1$ given by [30]

$$\varepsilon = \frac{1}{\sqrt{10^{-L_R/10} - 1}} \cdot \left| \frac{P_N(s)}{F_N(s)} \right|_{s=\pm 1}$$

where L_R is the return loss level in dB as defined in equation (4.10). It is assumed that polynomials $F(s)$, $P(s)$ and $E(s)$ are normalised such that their highest degree coefficients are unity.

For a 3-port power splitter consisting of tri-coupled resonators as described in figure 4.3, equation (4.14) may be extended to describe the reflection and transmission functions as follows [8]

$$S_{11}(s)=\frac{F(s)}{E(s)} \quad S_{21}(s)=\frac{P(s)}{\varepsilon_1 E(s)} \quad S_{31}(s)=\frac{P(s)}{\varepsilon_2 E(s)} \tag{4.15}$$

$F(s)$ and $E(s)$ are the 3rd order polynomials, and $E(s)$ has its complex roots corresponding to the filter pole positions. ε_1 and ε_2 are constants used to normalise $S_{21}(s)$ and $S_{31}(s)$, respectively. $E(s)$ can be constructed if $F(s)$, $E(s)$, ε_1 and ε_2 are known as in [8]. The expression for ε_1 and ε_2 is shown in [30] as

$$\varepsilon_1=\sqrt{\frac{1+\beta}{10^{-L_R/10}-1}}.\left|\frac{P(s)}{F(s)}\right|_{s=\pm j} \quad \varepsilon_2=\sqrt{\frac{1+\beta}{\beta\left(10^{-L_R/10}-1\right)}}.\left|\frac{P(s)}{F(s)}\right|_{s=\pm j} \tag{4.16}$$

where β is as in equation (4.8) in previous section.

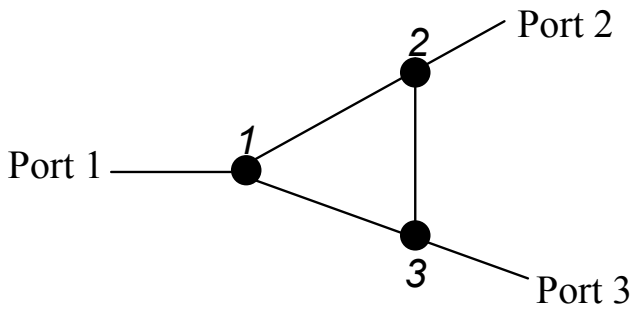

Figure 4.5 Topology of tri-resonator structure.

$P(s)$ corresponds to the frequency locations of the transmission zeros. It is the polynomial of order two because there are only two transmission zeros for the proposed tri-resonator structure with 3-ports as shown in figure 4.5. This is mathematically proven

and is presented in section 4.3.1.1. The solutions of $F(s)$ describes the locations of reflection zeros. In case of polynomial synthesis method, the reflection zeros can be computed by using Cameron's recursive technique as in [4], which will not be presented in this thesis. A new approach is used to develop a clear synthesis procedure to design a tri-coupled resonator power splitter consisting of only three resonators. To begin with, a set of simple formulae to compute the coupling coefficients and external quality factors are derived from reflection coefficient, S_{11} and transmission coefficients S_{21} and S_{31}. This technique is discussed further in the next section.

4.3. Coupling matrix Method for Designing Filters

Coupling coefficients of inter-coupled resonator filters and external quality factors of the input and output resonators are the basis for designing coupled resonator filters. Different techniques of designing microwave filters such as network synthesis, polynomial and coupling matrix synthesis method are presented in [2], [8], [11-13] and [17-18].

In this section practical filter design using normalised coupling matrix method will be explored. The design procedure starts with developing mathematical expressions to calculate the normalised coupling coefficients and the external quality factors using the general equations of S-parameters in equation (3.35).

4.3.1. Derivation of Reflection and Transmission zero locations for a 3x3 Normalised Coupling Matrix

The calculation of coupling parameters such as the normalised coupling coefficients and the external quality factors is an important step in this new design procedure. To realise the proposed tri-resonator structure shown in figure 4.6 analytically, a mathematical expression will be developed using the general 3×3 normalised coupling matrix, $[A]$ analogous to the normalised impedance matrix for the asynchronously tuned resonators shown in Chapter 3, equation 3.11. Thus, the normalised coupling matrix, $[A]$ is given by

$$[A]=\begin{bmatrix} \frac{1}{q_{e1}}+p-jm_{11} & -jm_{12} & -jm_{13} \\ -jm_{21} & \frac{1}{q_{e2}}+p-jm_{22} & -jm_{23} \\ -jm_{31} & -jm_{23} & \frac{1}{q_{e3}}+p-jm_{33} \end{bmatrix} \tag{4.17}$$

The general equation of S-parameters of a tri-coupled tri-resonator structure in terms of a 3×3 coupling matrix, $[A]$ is given in Chapter 3 in equation (3.35) and is presented here again as

$$S_{21}=2\frac{1}{\sqrt{q_{e1}q_{e2}}}[A]_{21}^{-1}$$

$$S_{31}=2\frac{1}{\sqrt{q_{e1}q_{e3}}}[A]_{31}^{-1} \tag{4.18}$$

$$S_{11}=1-\frac{2}{q_{e1}}[A]_{11}^{-1}$$

The variables q_{e1}, q_{e2} and q_{e3} are the external quality factors, $p = j\omega$ is the complex frequency variable, $[U]$ is the $n \times n$ identity matrix and $[m]$ is the normalised coupling matrix.

The inverse of a normalised coupling matrix in equation (4.18) can be described in terms of the adjugate and determinant of matrix $[A]$ as follows [12]

$$[A]^{-1} = \frac{adj([A])}{\det([A])}, \ \det([A]) \neq 0 \tag{4.19}$$

where $adj([A])$ is the adjugate of a square matrix $[A]$, and $\det([A])$ is its determinant. Noting that the adjugate of a matrix is the transpose of a matrix of cofactors created from a matrix, $[A]$. Thus, using this definition, equation (4.19) can be re-defined more precisely as

$$[A]^{-1}_{n1} = \frac{cof_{1n}([A])}{\det([A])}, \ \det([A]) \neq 0 \tag{4.20}$$

Where $[A]^{-1}_{n1}$ is the $(n,1)$ element value of the inverse matrix, $[A]$, and $cof_{1n}([A])$ is the $(1,n)$ element of the cofactor matrix, $[A]$ for $n = 1,\ 2$ and 3.

Making use of equation (4.20) and substituting into equation (4.18) yields

$$S_{21} = \frac{2}{\sqrt{(q_{e1}q_{e2})}} \cdot \frac{cof_{12}([A])}{\det([A])} \qquad S_{31} = \frac{2}{\sqrt{(q_{e1}q_{e3})}} \cdot \frac{cof_{13}([A])}{\det([A])}$$

$$S_{11} = 1 - \frac{2}{q_{e1}} \cdot \frac{cof_{11}([A])}{\det([A])} \tag{4.21}$$

4.3.1.1. Frequency Locations of Transmission zero

At a frequency location of transmission zero, equation (4.21) degenerates to zero, and shown as

$$S_{21}(\omega_4) = 0 \Rightarrow cof_{12}\left(\left[A(p)\right]\right) = 0$$
$$S_{31}(\omega_5) = 0 \Rightarrow cof_{13}\left(\left[A(p)\right]\right) = 0 \quad (4.22)$$

$$S_{11}(\omega_1, \omega_2, \omega_3) = 0 \Rightarrow 1 - \frac{2}{q_{e1}} \cdot \frac{cof_{11}\left(\left[A(p)\right]\right)}{\det\left(\left[A(p)\right]\right)} = 0 \quad (4.23)$$

where $p = j\omega_i$: ω_1, ω_2 and ω_3 are the frequency of reflection zero locations, ω_4 and ω_5 are normalised frequency of transmission zero for S_{21} and S_{31}, respectively.

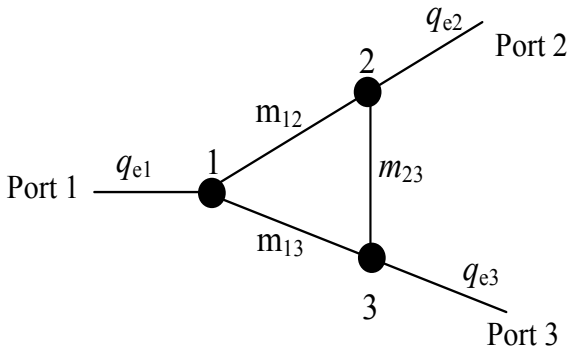

Figure 4.6: The proposed coupling structure for a tri-resonator showing couplings between each resonator.

It is assumed in figure 4.6 that port 1 is the input port coupled to resonator 1, and ports 2 and 3 are output ports coupled to resonators 2 and 3 respectively.

From equation (4.22), the $cof_{12}\left(\left[A(p)\right]\right)$ and $cof_{13}\left(\left[A(p)\right]\right)$ can be computed and shown as

$$\begin{aligned} cof_{12}\left(\left[A(p)\right]\right) &= -\left(-jm_{12}\left(-jm_{33}+p+\frac{1}{q_{e3}}\right)+m_{13}m_{23}\right)\Bigg|_{p=j\omega_4}=0 \\ cof_{13}\left(\left[A(p)\right]\right) &= -m_{12}m_{23}-\left(-jm_{13}\left(-jm_{22}+p+\frac{1}{q_{e2}}\right)\right)\Bigg|_{p=j\omega_5}=0 \end{aligned} \tag{4.24}$$

The detailed calculations are given in Appendix B. Rearranging equation (4.24) for the transmission zero locations for S_{21} and S_{31} yields

$$\begin{aligned} \omega_4 &= m_{33}-\frac{m_{13}m_{23}}{m_{12}}+j\frac{1}{q_{e3}} \\ \omega_5 &= m_{22}-\frac{m_{12}m_{23}}{m_{13}}+j\frac{1}{q_{e2}} \end{aligned} \tag{4.25}$$

For synchronously tuned filter, where $m_{11}=m_{22}=m_{33}=0$, equation (4.25) will further reduce to

$$\begin{aligned} \omega_4 &= -\frac{m_{13}m_{23}}{m_{12}}+j\frac{1}{q_{e3}} \\ \omega_5 &= -\frac{m_{12}m_{23}}{m_{13}}+j\frac{1}{q_{e2}} \end{aligned} \tag{4.26}$$

From equation (4.26) it may readily be seen that there are two transmissions zero locations for the proposed structure shown in figure 4.6 with all resonators are coupled to one another.

4.3.1.2. Frequency Locations of Reflection zeros

Similarly, we will continue to find $cof_{11}\left(\left[A(p)\right]\right)$ and $\det\left(\left[A(p)\right]\right)$ as a function of normalised coupling coefficients and external quality factors. Thus, from equation (4.23), the $cof_{11}\left(\left[A(p)\right]\right)$ is

$$cof_{11}\left(\left[A(p)\right]\right) = p^2 + \left(\frac{1}{q_{e3}} + \frac{1}{q_{e2}} - jm_{22} - jm_{33}\right)p + \frac{1}{q_{e2}q_{e3}} - m_{22}m_{33} + (m_{23})^2 - j\frac{m_{22}}{q_{e3}} - j\frac{m_{33}}{q_{e2}} \tag{4.27}$$

while the $\det\left(\left[A(p)\right]\right)$ is

$$\begin{aligned}\det\left[A(p)\right] = {} & jm_{11}m_{22}m_{33} - m_{11}m_{22}p - \frac{m_{11}m_{22}}{q_{e3}} - m_{11}m_{33}p - jm_{11}p^2 - \frac{jm_{11}p}{q_{e3}} \\ & - \frac{m_{11}m_{33}}{q_{e2}} - \frac{jm_{11}p}{q_{e2}} - \frac{jm_{11}}{q_{e2}q_{e3}} - jm_{11}\left(m_{23}\right)^2 - \frac{m_{22}m_{33}}{q_{e1}} - \frac{jm_{22}p}{q_{e1}} - \\ & \frac{jm_{22}}{q_{e1}q_{e3}} - \frac{jm_{33}p}{q_{e1}} + \frac{p^2}{q_{e1}} + \frac{p}{q_{e1}q_{e3}} - \frac{jm_{33}}{q_{e1}q_{e2}} + \frac{p}{q_{e1}q_{e2}} + \frac{1}{q_{e1}q_{e2}q_{e3}} + \\ & \frac{\left(m_{23}\right)^2}{q_{e1}} - m_{22}m_{33}p - jm_{22}p - \frac{jm_{22}p}{q_{e3}} - jm_{33}p^2 + p^3 + \frac{p^2}{q_{e3}} - \frac{jm_{33}p}{q_{e2}} + \\ & \frac{p^2}{q_{e2}} + \frac{p}{q_{e2}q_{e3}} + p\left(m_{23}\right)^2 - j(m_{12})^2 m_{33} + (m_{12})^2 p + \frac{(m_{12})^2}{q_{e3}} + \\ & j2m_{12}m_{13}m_{23} - j(m_{13})^2 m_{22} + (m_{13})^2 p + \frac{(m_{13})^2}{q_{e2}}\end{aligned} \tag{4.28}$$

The detailed derivation of $cof_{11}\left(\left[A(p)\right]\right)$ and $\det\left(\left[A(p)\right]\right)$ are shown in Appendix B.

Substituting equations (4.27) and (4.28) into equation (4.23), yields

$$S_{11}(j\omega_1, j\omega_2, j\omega_3) = p^3 + \left(\frac{1}{q_{e3}} + \frac{1}{q_{e2}} - \frac{1}{q_{e1}} - j\left(m_{11} + m_{22} + m_{33}\right)\right)p^2 +$$

$$\left(-m_{11}m_{22} - m_{11}m_{33} - m_{22}m_{33} + {m_{23}}^2 + (m_{12})^2 + {m_{13}}^2\right)p +$$

$$\left(-\frac{1}{q_{e1}q_{e2}} - \frac{1}{q_{e1}q_{e3}} + \frac{1}{q_{e2}q_{e3}}\right)p -$$

$$j\left(\frac{-m_{22} - m_{33}}{q_{e1}} + \frac{m_{11} + m_{33}}{q_{e2}} + \frac{m_{11} + m_{22}}{q_{e3}}\right)p +$$

$$\frac{m_{22}m_{33} - {m_{23}}^2}{q_{e1}} + \frac{{m_{13}}^2 - m_{11}m_{33}}{q_{e2}} + \frac{{m_{12}}^2 - m_{11}m_{22}}{q_{e3}} - \frac{1}{q_{e1}q_{e2}q_{e3}} -$$

$$j\left(\frac{m_{11}}{q_{e2}q_{e3}} - \frac{m_{22}}{q_{e1}q_{e3}} - \frac{m_{33}}{q_{e1}q_{e2}} + m_{11}{m_{23}}^2 + m_{22}{m_{13}}^2\right) + \qquad (4.29)$$

$$j\left(m_{33}{m_{12}}^2 - 2m_{13}m_{12}m_{23} - m_{11}m_{22}m_{33}\right) = 0$$

Equation (4.29) is the general expression to compute reflection zero locations for asynchronously tuned tri-coupled tri-resonator filter structure shown in figure (4.6). It is also applicable for synchronously tuned tri-resonator filters with the assumption that no self couplings are considered, that is for $m_{11} = m_{22} = m_{33} = 0$. It is worth mentioning that there are 12 unknown parameters in equation (4.29). These are 6 normalised coupling coefficients ($m_{11}, m_{12}, m_{13}, m_{22}, m_{23}, m_{33}$), 3 scaled external quality factors (q_{e1}, q_{e2} and q_{e3}) and 3 reflection zero locations (p_1, p_2 and p_3).

A complete solution will be sought to fully realise the proposed tri-coupled tri-resonator structure. To find these analytically, mathematical manipulations of equation (4.29) along with some assumptions are further explored and presented in chapter 5 in detail.

By defining

$$a = \left(\frac{1}{q_{e3}} + \frac{1}{q_{e2}} - \frac{1}{q_{e1}} \right) - j\left(m_{11} + m_{22} + m_{33} \right) \tag{4.30}$$

$$b = -m_{11}m_{22} - m_{11}m_{33} - m_{22}m_{33} + m_{23}{}^2 +$$

$$(m_{12})^2 + m_{13}{}^2 - \frac{1}{q_{e1}q_{e2}} - \frac{1}{q_{e1}q_{e3}} + \frac{1}{q_{e2}q_{e3}} - \tag{4.31}$$

$$j\left(\frac{-m_{22} - m_{33}}{q_{e1}} + \frac{m_{11} + m_{33}}{q_{e2}} + \frac{m_{11} + m_{22}}{q_{e3}} \right)$$

and

$$c = \frac{m_{22}m_{33} - m_{23}{}^2}{q_{e1}} + \frac{m_{13}{}^2 - m_{11}m_{33}}{q_{e2}} + \frac{m_{12}{}^2 - m_{11}m_{22}}{q_{e3}} - \frac{1}{q_{e1}q_{e2}q_{e3}}$$

$$- j\left(\frac{m_{11}}{q_{e2}q_{e3}} - \frac{m_{22}}{q_{e1}q_{e3}} - \frac{m_{33}}{q_{e1}q_{e2}} + m_{11}m_{23}{}^2 + m_{22}m_{13}{}^2 \right) - \tag{4.32}$$

$$j\left(m_{33}m_{12}{}^2 - 2m_{13}m_{12}m_{23} - m_{11}m_{22}m_{33} \right)$$

equation (4.29) can be rewritten

$$S_{11}(p) = f(p) = p^3 + ap^2 + bp + c = 0 \tag{4.33}$$

The solution to this equation is what we require. This is given in Appendix A. It is clear that this is a very complex to solve for the zeros of this function which is shown in Appendix A. To simplify the problem, the cubic equation can be written in terms of the three solutions as

$$\begin{aligned} S_{11}(p_1) &= p_1^3 + ap_1^2 + bp_1 + c = 0 \\ S_{11}(p_2) &= p_2^3 + ap_2^2 + bp_2 + c = 0 \\ S_{11}(p_3) &= p_3^3 + ap_3^2 + bp_3 + c = 0 \end{aligned} \tag{4.34}$$

Where p_1, p_2 and p_3 are the zeros of (4.33) and the frequency locations of the reflection zeros.

Now we can guess the frequency locations of the reflection zeros in order to avoid the complexity. $p_1 = j\omega_1$, $p_2 = j\omega_2$ and $p_3 = j\omega_3$, where $\omega_1 = 1, \omega_2 = 0$ and $\omega_3 = -1$ are put a first step in the process of trying to simplify the problem. There are of course no reasons why these should be solutions of (4.33), but we will continue to investigate. Thus, mathematical analysis in chapter 5 is based on these values of reflection zeros.

It should be pointed out that for the examples presented in this thesis, the responses of the tri-resonator structures are not conventionally normalised, i.e., the cut off frequency is not ±1 rad/sec. However, these responses can be easily transformed (or normalised) simply by

multiplying a constant with all the coupling coefficients of the coupling matrices to renormalize the bandpass edge to ±1 rad/sec. This will of course make $\omega_1 < 1$ and $\omega_3 > -1$. Using these values in (4.33) will give us

$$\sum S_{11}\left(p_{1,2,3}\right) = 0$$

$$S_{11}\left(-j, 0, j\right) = -2a + 3c \tag{4.35}$$

Substituting for a and c in (4.34) gives the following expression

$$S_{11}\left(-j,0,j\right) = -2\left(\frac{1}{q_{e3}} + \frac{1}{q_{e2}} - \frac{1}{q_{e1}} - j\left(m_{11} + m_{22} + m_{33}\right)\right) +$$

$$3\left(\frac{m_{22}m_{33} - m_{23}^{\ 2}}{q_{e1}} + \frac{m_{13}^{\ 2} - m_{11}m_{33}}{q_{e2}} + \frac{m_{12}^{\ 2} - m_{11}m_{22}}{q_{e3}} - \frac{1}{q_{e1}q_{e2}q_{e3}}\right) -$$

$$j3\left(\frac{m_{11}}{q_{e2}q_{e3}} - \frac{m_{22}}{q_{e1}q_{e3}} - \frac{m_{33}}{q_{e1}q_{e2}} + m_{11}m_{23}^{\ 2} + m_{22}m_{13}^{\ 2} + m_{33}m_{12}^{\ 2} - 2m_{13}m_{12}m_{23} - m_{11}m_{22}m_{33}\right) = 0 \tag{4.36}$$

From equation (4.25)

$$m_{23} = \frac{m_{12}}{m_{13}}\left(m_{33} - \omega_4 + j\frac{1}{q_{e3}}\right) \tag{4.37}$$

or

$$m_{23} = \frac{m_{13}}{m_{12}}\left(m_{22} - \omega_5 + j\frac{1}{q_{e2}} \right) \tag{4.38}$$

Note that equations (4.37) and (4.38) are equal. The back substitution of these equations into equation (4.33) will further simplify the expression. We have now setup the solution and manipulations of this will be seen in the next chapter. In the process of designing 3-dB tri-resonator power splitter, the analysis and application of equation (4.33) or (4.30) are also presented in the next chapter.

Chapter 5

Microwave Tri-resonator Filter Structure

5.1. 3-dB Tri-resonator Power Splitter Coupling Matrix Synthesis

The lowpass prototype design of a 3-dB power splitter is presented in this section. The power splitter frequency response is assumed to be symmetrical. For a symmetrical frequency response an equal power division between output ports 2 and 3 is considered. This is illustrated analytically, and the design parameters for a 3-dB tri-resonator power splitter are calculated. For the practical design, the following assumptions are made and used throughout a mathematical analysis to calculate the normalised coupling coefficients and external quality factors for splitter design.

5.1.1. Design procedure for Power Splitter with no Coupling between Resonators 2 and 3

Consider the following assumptions and the topology shown in figure 5.1.

$$m_{11} = m_{22} = m_{33} = 0,\ m_{12} = m_{13},\ m_{23} = 0,\ \ q_{e2} = q_{e3} = q_e^{'} \tag{5.1}$$

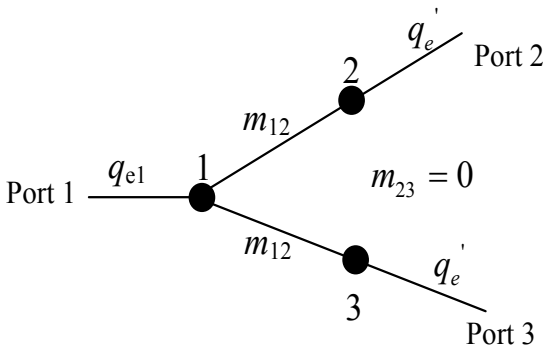

Figure 5.1: 3-dB power divider topology with output ports 2 and 3 are uncoupled

These assumptions will transform the topology proposed for tri-coupled tri-resonator structure shown in chapter 4, figure 4.6 into tri-resonator power splitter structure as shown in figure 5.1.

Based on the assumptions, there are only two possible reflection zeros for the topology shown in figure 5.1. The same values of frequency locations of reflection zeros used in equation (4.34) can also be assumed here but using $p_2 = j\omega_2$, where $\omega_2 = 0$ into equation (4.34) gives non-zero value. This value is said to be the peak value of the return loss, r of the response.

Thus recalling equation (4.32), and using $p_1 = -j$, $p_2 = 0$ and $p_3 = j$, into it yields

$$S_{11}(p_1 = -j) = j - a - jb + c = 0 \tag{5.2}$$

$$S_{11}(p_2 = 0) = c = r \tag{5.3}$$

$$S_{11}(p_3 = j) = -j - a + jb + c = 0 \tag{5.4}$$

where $r = 10^{\frac{-L_R}{20}}$ in linear form, and L_R in dB-scale and should be in the range of $0 \le L_R \le \infty$.

Taking the summation of equation (5.2) and (5.4) gives

$$-a + c = 0 \tag{5.5}$$

By using the assumptions in equation (5.1) into equation (4.30-4.32) in chapter 4, the parameters a and c can be shown as

$$a = -\frac{1}{q_{e1}} + \frac{2}{q_e^{'}}, \quad c = \frac{2m_{12}^{\ 2}}{q_e^{'}} - \frac{1}{q_{e1}q_e^{'2}} \tag{5.6}$$

Substitution of equation (5.6) into equation (5.5), and making some mathematical manipulations give

$$m_{12} = m_{13} = \pm\sqrt{\frac{1}{2q_{e1}}\left(\frac{1}{q_e^{'}} - q_e^{'}\right)+1} \tag{5.7}$$

By assuming values for q_{e1} and $q_e^{'}$, and using them into equation (5.7), range of values for m_{12} and m_{13} can be calculated. Assumed values of q_{e1} and $q_e^{'}$, and calculated values of m_{12} and m_{13} are summarised in table 5.1. By using the values in this table, the corresponding symmetric frequency responses of 3-dB tri-resonator power splitters at different return losses are realised and shown in figure 5.2.

Table 5.1 Normalised coupling coefficients and external quality factors: calculated

q_{e1}	0.10	0.25	0.35	0.475	0.50	0.55	0.60	0.65	0.70	0.75	0.85	0.90	0.95	1.0	1.25
$q_e^{'}$	0.10	0.25	0.35	0.475	0.50	0.55	0.60	0.65	0.70	0.75	0.85	0.90	0.95	1.0	1.25
$m_{12} = m_{13}$	7.1064	2.9155	2.1405	1.6480	1.5811	1.4673	1.3744	1.2975	1.2330	1.1785	1.091	1.0570	1.0267	1.0	0.9055

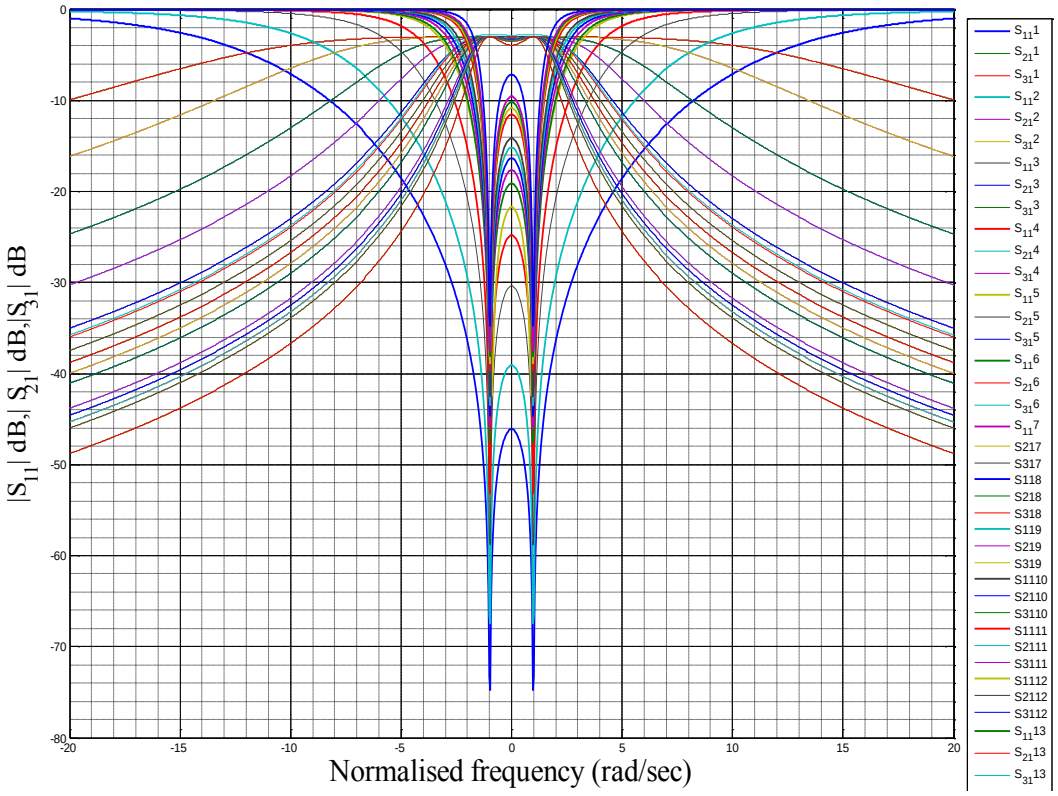

Figure 5.2 Frequency responses of a 3-dB tri-resonator power splitter for the topology shown in figure 5.1.

Figure 5.2 demonstrates various splitter responses at reflection zeros of $\pm j$ with different reflection losses. The reflection zero locations have been forced to be $\pm j$ as it has been explained in the mathematical derivation to calculate the normalised coupling coefficients and external quality factors in chapter 4, section 4.3.1.2.

By referring to table 5.1, one can design a 3-dB tri-resonator power splitter with a goal of specific return loss (RL). For instance, if we want to realise a symmetric frequency response of 3-dB tri-resonator power splitter at 20 dB return loss, the normalised coupling coefficients, m_{12} and m_{13}, and external quality factors, q_{e1} and $q_e^{'}$ can be read from table

5.1 as q_{e1}=$q_e^{'}$=0.475 and m_{12}=m_{13}=1.6480.The frequency response for this particular values is given in figure 5.3.

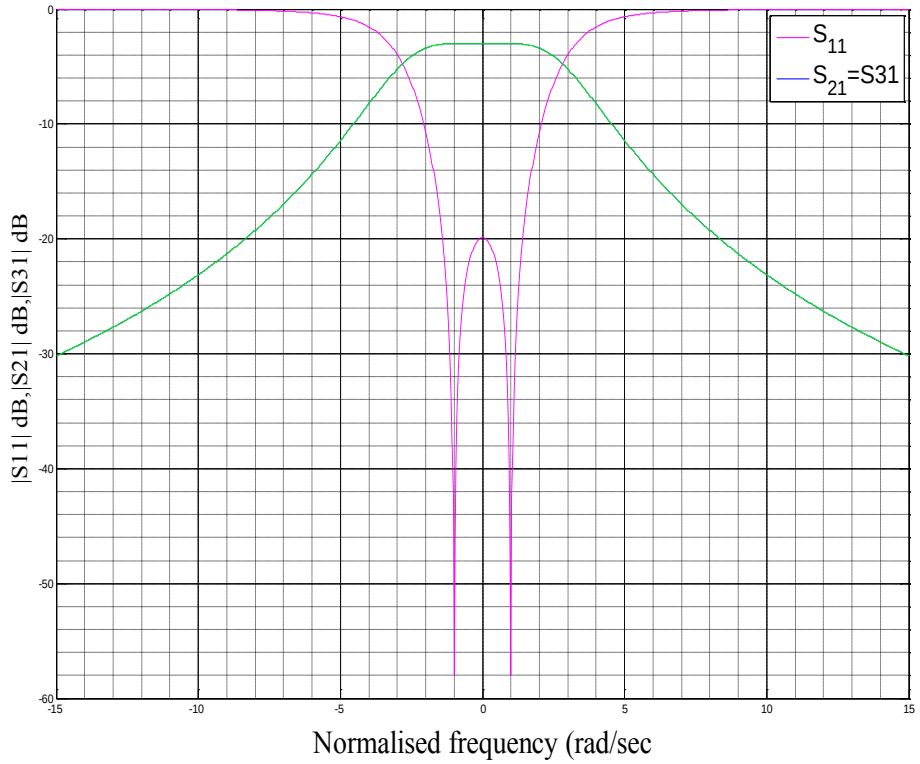

Figure 5.3 A 3-dB power splitter response at -20 dB return loss

To investigate the return loss, r equations (5.2-5.4) are further simultaneously computed as follows:

Subtracting equation (5.2) with equation (5.3) yields

$$j - a - jb = -r \tag{5.8}$$

and subtracting equation (5.3) from equation (5.4) gives

$$j + a - jb = r \tag{5.9}$$

Solving equation (5.8) and (5.9) simultaneously gives $b=1$, and using this into (5.8) yields $a=r$. Also it is clear from equation (5.3) that $c=r$. Thus a, r and c are related as

$$a=r=c \tag{5.10}$$

Recalling the definitions of a, b and c in equations (4.28-4.30), and making use of equation (5.1) into them may give the following expressions for a, b and c as

$$a=-\frac{1}{q_{e1}}+\frac{2}{q_e^{'}},\quad c=\frac{2m_{12}^{\ 2}}{q_e^{'}}-\frac{1}{q_{e1}q_e^{'2}} \tag{5.11}$$

$$b=2m_{12}^{\ 2}-\frac{2}{q_{e1}q_e^{'}}+\frac{1}{q_e^{'2}} \tag{5.12}$$

Substitution of equation (5.11) into (5.10) gives

$$-\frac{q_e^{'}}{q_1}+2=2m_{12}^{\ 2}-\frac{1}{q_1q_e^{'}}=r$$

$$\Rightarrow r=2m_{12}^{\ 2}-\frac{1}{q_1q_e^{'}} \tag{5.13}$$

Using $b=1$ in equation (5.12), and making $m_{12}^{\ 2}$ a subject yields

$$m_{12}^{\ 2}=\frac{1}{2}\left(\frac{2}{q_{e1}q_e^{'}}-\frac{1}{q_e^{'2}}+1\right) \tag{5.14}$$

Substitution of equation (5.14) into equation (5.13) gives the return loss as a function of normalised external quality factors. This is shown as

$$r = \frac{1}{q_e^{'2}}\left(-\frac{1}{q_e^{'}} + \frac{1}{q_{e1}}\right) + \frac{1}{q_e^{'}} \tag{5.15}$$

It should be noted that the return loss lies in the range of $0 \le r \le 1$ for passive circuit or in the range of negative infinity to zero in the dB-scale; i.e., $-\infty \le RL \le 0$ dB.

The graph of return loss versus the external quality factor, q_{e2} and q_{e3} at the output ports 2 and 3 respectively is presented in figure 5.4. For the sake of clarity, the relationship between q_{e1} and $q_e^{'}$ is given by $q_{e1} = \alpha q_e^{'}$ where $0.15 \le \alpha \le 1$ is considered and shown as a non-parabolic part of figure 5.4 for the range of $0 \le r \le 1$. However, for $1.25 < \alpha \le 6.25$, the return loss responses are parabolic as elaborated in figure 5.4.

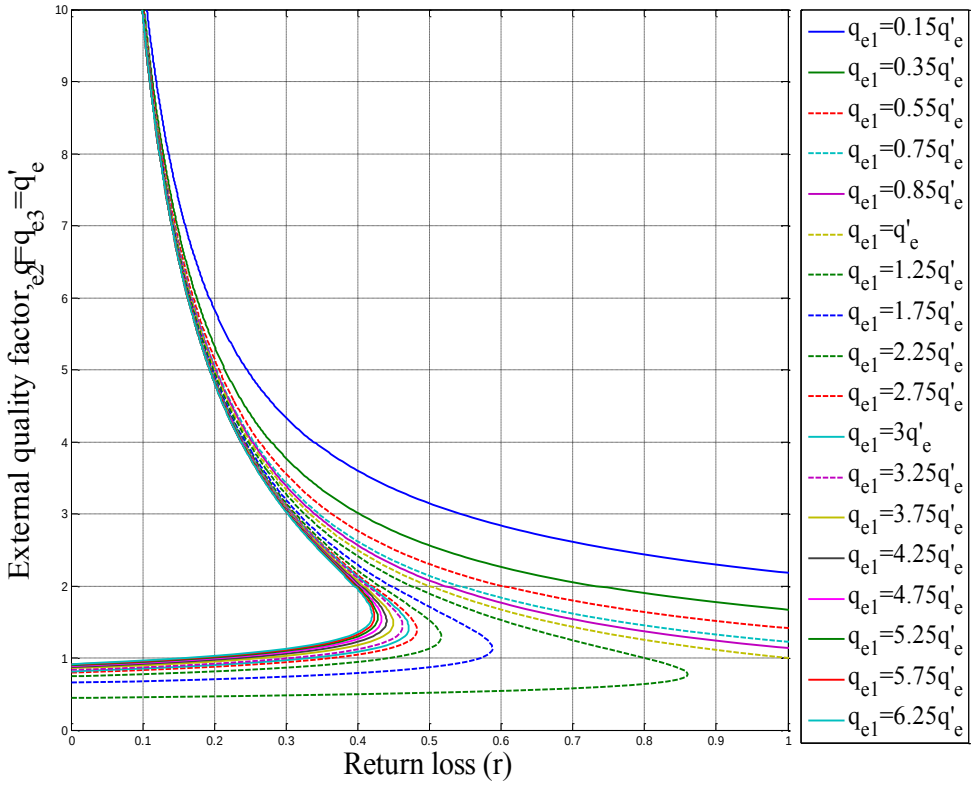

Figure 5.4 External quality factors versus, r, for $q_{e1} = \alpha q_e^{'}$ where $0.15 \le \alpha \le 6.25$

From figure 5.4, it can be seen that an infinite number of external quality factors at the output ports can be collected at a desired ripple value. For a specific return loss value, two different values of $q_e^{'}$ can be read. This is because of the parabolic nature of the graphs in figure 5.4 for the case when $1.25 \le \alpha \le 6.25$ is considered. For instance, for the case $q_{e1} = 1.25 q_e^{'}$ in figure 5.4, at a particular value of r, say $r = 0.25$, $q_e^{'}$ has two values, and may be read as 0.49 and 4.0. At these two values of $q_e^{'}$, there are two corresponding values of normalised coupling coefficients, m_{12} where $m_{12} = m_{13}$ in figure 5.5, and this is consistent with equation (5.7); i.e., $m_{12} = m_{13}$ can be negative or positive values.

Using the appropriate values of $q_e^{'}$ from figure 5.4 at a particular return loss, r, and the corresponding values of coupling coefficients from figure 5.5, a 3-dB power splitter parameters can be determined. Figure 5.5 shows the external quality factors versus the positive coupling coefficients. For the negative coupling coefficients, $m_{12} = m_{13}$ versus external quality factor can be drawn simply by taking the mirror image of figure 5.5, and hence, the negative values of $m_{12} = m_{13}$ can be extracted. These illustrate that m_{12} and m_{13} hold negative or positive values as discussed and has also been analytically proven and shown in equation (5.7).

It should be noted that the mirror image of figure 5.5 which gives rise to the negative values of coupling coefficients does not mean that the negative values of coupling coefficients give rise to an image frequency response of the splitter. Instead, the positive and negative values of m_{12} and m_{13} give same symmetric frequency response of 3-dB tri-resonator power splitters and this is presented in the next section as examples.

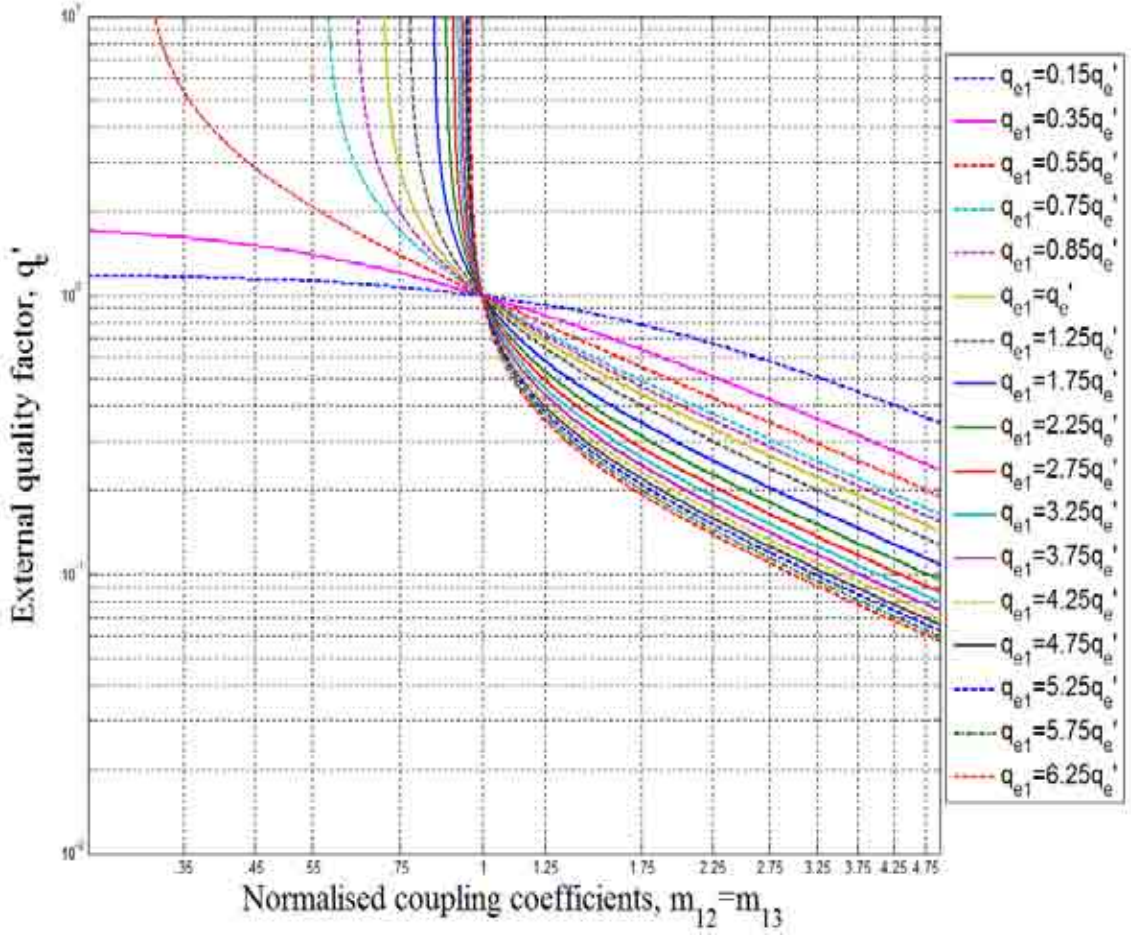

Figure 5.5 The relationship between normalised coupling coefficients and external quality factors for $m_{12} = m_{13} > 0$ in log scale.

The response in figure 5.5 describes the degree of freedom in reading multiple values of m_{12} and m_{13} for a corresponding values of $q_e^{'}$ directly from it. Besides this, we can have 3-dB tri-resonator power splitter of identical responses with diferent values of coupling coefficients and external qaulity factors. These responses are shown in the design examples 1 and 2 in the next section. It can be noted from figure 5.5 that; at a point $(1,\ 1)$, the responses of the coupling coefficients, m intersect.

The design procedure can be summarised in 4 steps as follows:

1. Determine the return loss , r from figure 5.4
2. Read the values of external quality factors from figure 5.4 at input port 1 and output ports 2 and 3
3. For the corresponding values of $q_e^{'}$ in figure 5.4, read the corresponding values of coupling coefficients from figure 5.5
4. Determine the response of the power splitter topology shown in figure 5.1

5.1.2 Coupling Matrix Power Divider Examples

Using the design procedure outlined the following 3-dB tri-resonator power splitters are designed and presented. The normalised coupling matrix and external quality factors illustrated in examples 1 and 2 are extracted from figure 5.5. These are some of the values we are interested in for the design purpose to get better responses. It is also interesting to note that the coupling matrices and external quality factors demonstrated in design examples 1 and 2 can also be calculated using equation 5.7, and found to be consistent with the values from the graph of coupling coefficients versus $q_e^{'}$-factor as expected.

The intention in the design examples 1 and 2 is to show how two different coupling matrices and external quality factors can be used to design same tri-resonator power splitter responses.

Design Example 1:

In this example, two different normalised coupling matrices and external quality factors are used to give exactly the same response with a return loss of 20.33 dB as shown in

figures 5.6 and 5.6. This is possible as the graph in figure 5.4 is parabolic and two values of normalised external quality factors for a single value of return loss can be obtained.

$$m = \begin{bmatrix} 0 & \pm 1.6875 & \pm 1.6875 \\ \pm 1.6875 & 0 & 0 \\ \pm 1.6875 & 0 & 0 \end{bmatrix}$$

$$q_{e1} = 0.4615 = q_e'$$

(a)

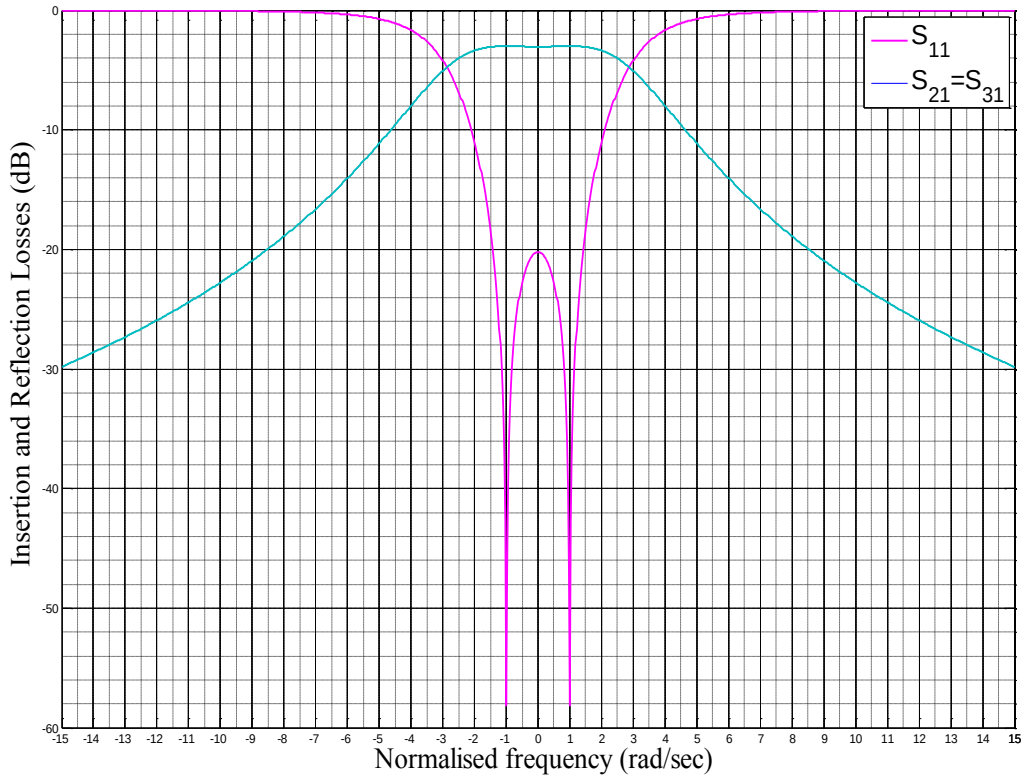

(b)

Figure 5.6 (a) Normalised coupling matrix and external quality factors and (b) A 3-dB tri-resonator power splitter with the bandpass edge of ±1.45 rad/s.

$$m = \begin{bmatrix} 0 & \pm 1.6799 & \pm 1.6799 \\ \pm 1.6799 & 0 & 0 \\ \pm 1.6799 & 0 & 0 \end{bmatrix}, \; q_{e1} = q_e^{'} = 0.4640$$

(a)

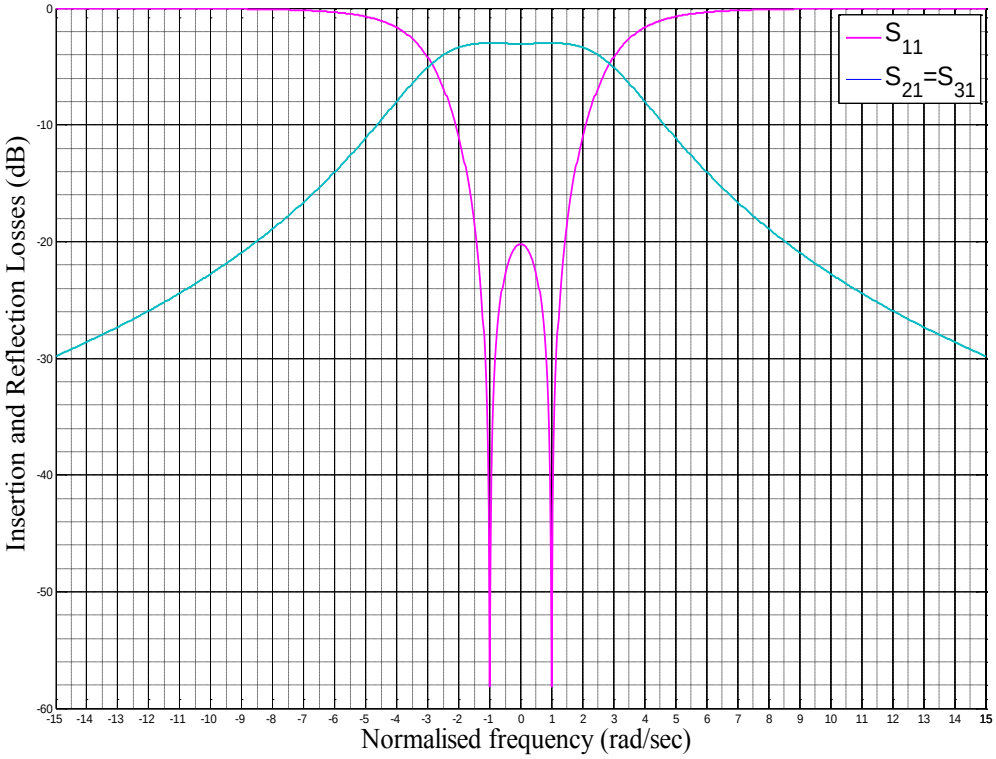

(b)

Figure 5.7 (a) Normalised coupling matrix and external quality factors and (b) A 3-dB tri-resonator power splitter with the bandpass edge of ±1.45 rad/s.

The tri-resonator power splitter responses shown in figure 5.6 and 5.7 are the same as expected except that the normalised coupling matrices and external quality factors obtained are different. The two graphs are therefore, evident that exactly the same responses of a tri-resonator power splitter can be designed using two different normalised coupling matrices and external quality factors as discussed above in this section. The power splitter responses in figure 5.6 and 5.7 have the same bandwidths. This is the case

as their bandpass edges are equal and is ±1.45 rad/sec. Thus, both splitters have bandwidth of 2.9 rad/sec.

Design Example 2:

In a similar way to design example 1, there are two distinct coupling matrices and external quality factors that yield same 3-dB tri-resonator power splitter with a return loss goal of 21.75 dB as shown in figures 5.8 and 5.9. These responses are obtained by using the two different coupling coefficients and external quality factors, and compared with each other.

$$m = \begin{bmatrix} 0 & \pm 1.8191 & \pm 1.8191 \\ \pm 1.8191 & 0 & 0 \\ \pm 1.8191 & 0 & 0 \end{bmatrix}, \quad q_{e1} = 0.4219 = q_e'$$

(a)

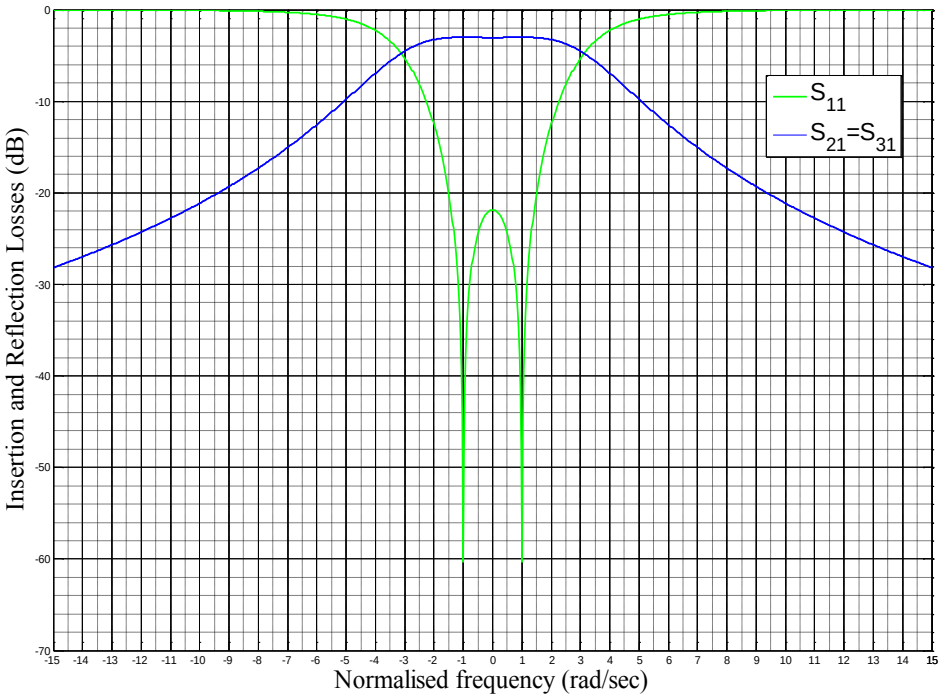

(b)

Figure 5.8 (a) Normalised coupling matrix and external quality factors and (b) Response of a 3-dB tri-resonator power splitter with the bandpass edge of ±1.5rad/s.

$$m = \begin{bmatrix} 0 & \pm 1.832 & \pm 1.832 \\ \pm 1.832 & 0 & 0 \\ \pm 1.832 & 0 & 0 \end{bmatrix}$$

$$q_{e1} = 0.4184 = q_e'$$

(a)

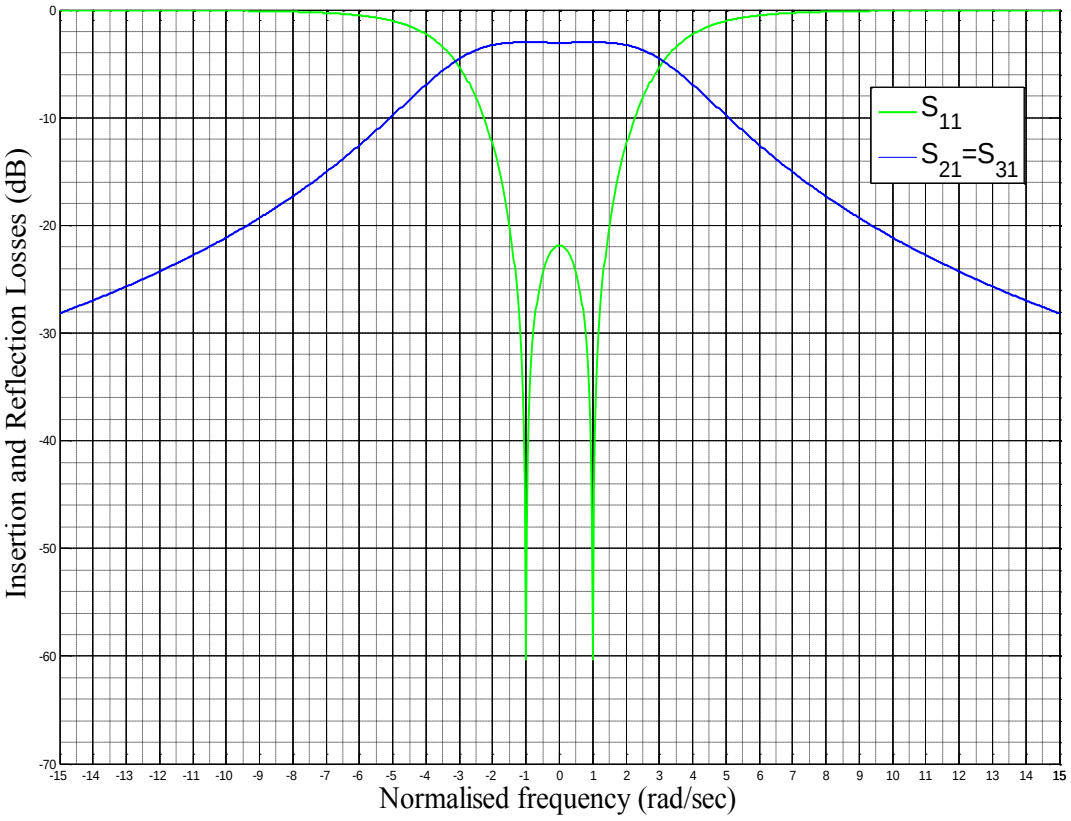

(b)

Figure 5.9 (a) Normalised coupling matrix and external quality factors and (b) Response of a 3-dB tri-resonator power splitter with the bandpass edge of ±1.5 rad/sec.

It can be seen from example 1 and 2 that the same 3-dB tri-resonator power splitter of identical response has been designed with different normalised coupling coefficients and external quality factors as explained earlier in this section.

The bandwidth of the power splitter responses shown in figure 5.8 and 5.9 are the same as they have the same bandpass edge, i.e., ±1.5 rad/sec.

From the design examples, it can be concluded that the range of values of coupling matrix and external quality factors can be calculated to design power splitters of identical responses.

In both design examples, the 3-dB tri-resonator power splitters having only one pair of transmission zeros have been designed.

5.2. Trisection Filter

A trisection filters comprise three couplings between three sequentially-numbered resonator filters. The first and third of which may be source or load terminals or it might be embedded within the coupling matrix of a higher-degree network [1]. As shown in figure 4.14, trisections are able to realize one transmission zero, and this is analytically proved in the next section. Figure 5.14 shows topology of trisection filter with the cross coupling between resonators 1 and 3, where it is assumed that the input and output ports are coupled to resonators 1 and 3 respectively. The cross coupling between resonators along with other couplings gives controllable transmission zero. We will see this shortly in this section when we work on the mathematical analysis of designing a trisection filter.

The placement of transmission zero is determined by the polarity of the cross coupling between resonator 1 and 3. The topology of the coupling arrangement is shown in figure 5.10.

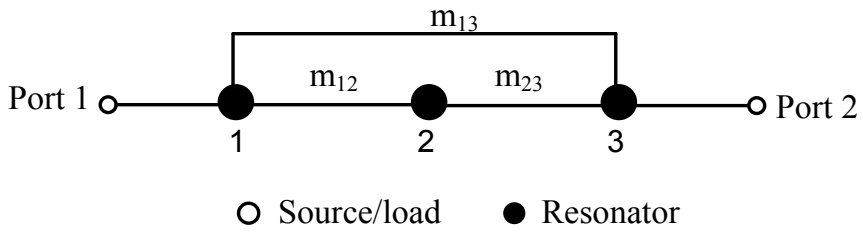

Figure 5.10 A tri-section filter showing the coupling between each resonator.

The direct and cross coupling phenomenon shown in figure 5.10 may be illustrated as follows:

m_{12} represents the direct coupling between resonators 1 and 2, m_{13} describes the cross coupling between resonators 1 and 3 and m_{23} stands for the main coupling between resonators 2 and 3.

The ability to realise just one transmission zero at finite frequency, makes the trisection filter very useful in synthesising filters with asymmetric characteristics. Trisection filters can exist either as a stand-alone within the network or multiply as a cascade. We will investigate a trisection filter with the type of topology shown in figure 5.10. We will not go further for multiple trisection filters which exist as cascaded within a network.

5.2.1. Analysis

Putting q_{e2} to infinity at port two of a three port tri-section filters topology described in figure 4.6 gives tri-coupled trisection filter structure shown in figure 5.10. This will transform the 3-port tri-resonator structure into two ports (input and output ports).

For a two port network the reflection and transmission S-parameters are given by

$$S_{11} = 1 - \frac{2}{q_{e1}}\left[\overline{A}\right]_{11}^{-1} = 1 - \frac{2}{q_{e1}} \cdot \frac{cof_{11}\left([A]\right)}{\det\left([A]\right)}$$
$$S_{21} = 2\frac{1}{\sqrt{q_{e1}q_{e3}}}\left[\overline{A}\right]_{31}^{-1} = \frac{2}{\sqrt{\left(q_{e1}q_{e3}\right)}} \cdot \frac{cof_{13}\left([A]\right)}{\det\left([A]\right)} \tag{5.16}$$

The transmission zero location may be found from equation (4.26). This may be shown as

$$\omega = m_{22} - \frac{m_{12}m_{23}}{m_{13}} \text{ for } q_{e2} \to \infty \tag{5.17}$$

where ω is the transmission zero.

A trisection filter requires the resonators to be asynchronously tuned to give an asymmetric filter frequency response [1]. Thus the resonating frequency for each resonator may be different. It will have an attenuation pole at one side of the passband.

To keep the physical configuration of the filter symmetrical even though the frequency response is asymmetric, the following assumptions are made [1]

$$m_{12} = m_{23},\ q_{e1} = q_{e3} = q_e^{"},\ \omega_{01} = \omega_{03} \tag{5.18}$$

where ω_{01} and ω_{03} are the angular frequencies of resonator 1 and 3, respectively.

Using these assumptions and $q_{e2} \to \infty$ in equation (4.32) yields

$$S_{11}(-j,0,j) = -2\left(-j\left(m_{11}+m_{22}+m_{33}\right)\right) + \frac{3}{q_e^{"}}\left(m_{22}m_{33} - m_{11}m_{22}\right) - j3\left(-\frac{m_{22}}{q_e^{"2}} + m_{12}{}^2\left(m_{11}+m_{33}-2m_{13}\right) + m_{22}m_{13}{}^2 - m_{11}m_{22}m_{33}\right) = 0 \tag{5.19}$$

Equation (5.17) may be re-arranged for m_{12} and shown by

$$m_{12}{}^2 = m_{13}\left(m_{22} - \omega\right) \tag{5.20}$$

Substitution of equation (5.20) into (5.19) gives the general expression as the function of transmission zero location, ω at reflection zeros, $-j, 0$ and j, and presented as

$$S_{11}(-j,0,j) = -2\left(-j\left(m_{11}+m_{22}+m_{33}\right)\right) + \frac{3}{q_e^{"}}\left(m_{22}m_{33} - m_{11}m_{22}\right) - j3\left(m_{22}m_{13}{}^2 - m_{11}m_{22}m_{33} - \frac{m_{22}}{q_e^{"2}}\right) + j3m_{13}\left(m_{22}-\omega\right)\left(m_{11}+m_{33}-2m_{13}\right) = 0 \tag{5.21}$$

This calculation can be taken one stage forward if $m_{11} = m_{33}$ is assumed, and substituted into equation (5.21). Thus, shown as

$$-2\left(-j\left(2m_{11}+m_{22}\right)\right)-j3\left(2m_{13}\left(m_{22}-\omega\right)\left(m_{11}-m_{13}\right)\right)- \\ j3\left(m_{22}m_{13}{}^{2}-m_{11}{}^{2}m_{22}\right)+j\frac{3m_{22}}{q_{e}^{"2}}=0 \tag{5.22}$$

To have same return loss level (or equal ripple) design, the following mathematical manipulations are carried out:

The first derivative of equation (4.33) is set to zero, and the peak frequency values of S_{11} in the passband may be computed as

$$\frac{d}{dp}\left(S_{11}\left(p\right)\right)=0\Rightarrow\frac{d}{dp}\left(p^{3}+ap^{2}+bp+c\right)=0$$
$$3p^{2}+2ap+b=0\Rightarrow p^{2}+\frac{2a}{3}p=-\frac{b}{3}$$

where a, b and c are coefficients of the cubic function as defined in equations (4.30-4.32).

The roots of p can be found by completing the square method, and given as

$$p=\frac{-a\pm\sqrt{\left(a^{2}-3b\right)}}{3} \tag{5.23}$$

Two peak frequency values can be picked up from equation (5.21), and these are given as

$$s_{r1} = -j\left(\frac{-a+\sqrt{\left(a^2-3b\right)}}{3}\right) \qquad s_{r2} = -j\left(\frac{-a-\sqrt{\left(a^2-3b\right)}}{3}\right)$$

The locations of these two peak frequency at which the return loss response will have equiripple values are demonstrated in figure 5.11.

For $q_2 \to \infty, m_{12} = m_{23}$ and $m_{11} = m_{33}$, the parameters a, b and c are given as

$$a = -j\left(2m_{11} + m_{22}\right)$$
$$b = \left(-2m_{11}m_{22} - m_{11}{}^2 + 2m_{12}{}^2 + (m_{13})^2 - \frac{2}{q^{"2}}\right)$$
$$c = -j\left(2m_{13}\left(m_{22}-\omega\right)\left(m_{11}-m_{13}\right) + m_{22}\left(m_{13}{}^2 - m_{11}{}^2 - \frac{1}{q^{"2}}\right)\right)$$

Now evaluating S_{11} at s_{r1} and s_{r2} gives return loss value r, where $r = 10^{\frac{-RL}{20}}$ for $0 < RL < \infty$ dB. This is shown as

$$S\left(s_{r1}\right) = r,\ \ S\left(s_{r2}\right) = r \ \Rightarrow S\left(s_{r1}\right) - r = 0,\ \ S\left(s_{r2}\right) - r = 0$$

$$\Rightarrow S\left(s_{r1}\right) - 10^{\frac{-RL}{20}} = 0,\ \ S\left(s_{r2}\right) - 10^{\frac{-RL}{20}} = 0 \qquad (5.24)$$

Or equation (5.23) can be generalised as

$$\sum_{i=1}^{2}\left|\left|S_{11(sri)}\right| - 10^{\frac{-RL}{20}}\right| = 0 \qquad (5.25)$$

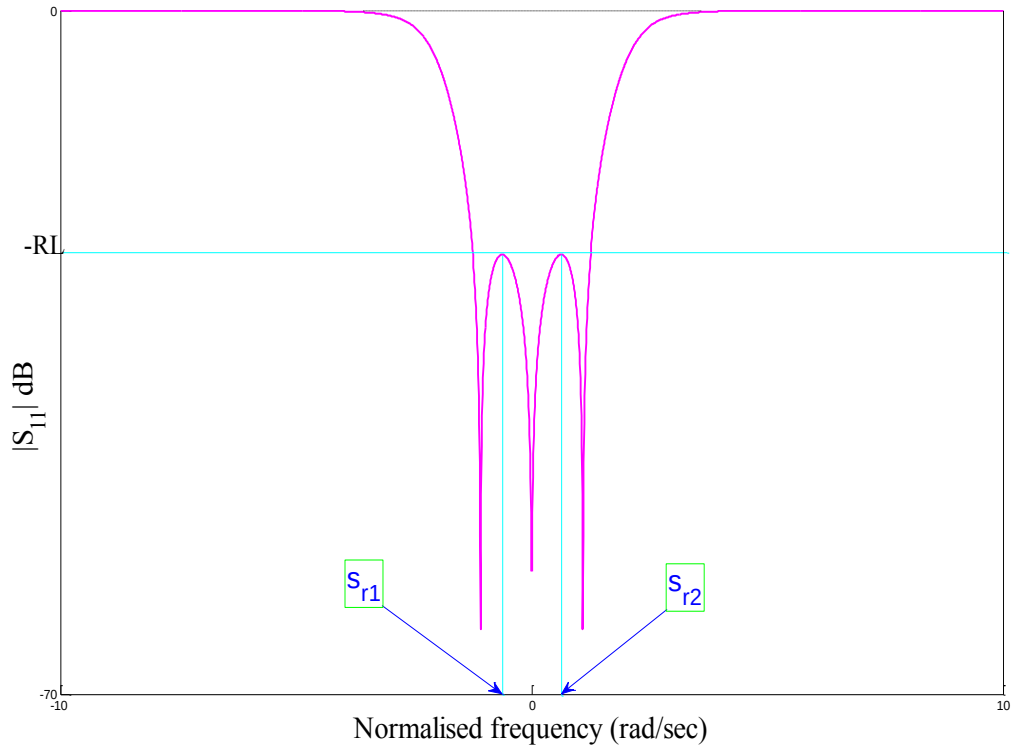

Figure 5.11 Return loss response with 3-reflection zeros and 2-frequency peaks showing equiripple level.

Adding equation (5.25) to equation (5.22) gives equation (5.26). Thus, the general formulation for the design of equiripple trisection filter of the topology shown in Figure 5.10 can be given as

$$-2\left(-j\left(2m_{11}+m_{22}\right)\right)-j3\left(2m_{13}\left(m_{22}-\omega\right)\left(m_{11}-m_{13}\right)+m_{22}\left(m_{13}{}^{2}-m_{11}{}^{2}-\frac{1}{q_{e}^{"2}}\right)\right)$$

$$+\sum_{i=1}^{2}\left|\left|S_{11(sri)}\right|-10^{\frac{-RL}{20}}\right|=0 \tag{5.26}$$

It is evident from the mathematical function in equation (5.26) that there are only 3 unknown normalised coupling coefficients, m_{11}, m_{22} and m_{13}, and an external quality factor, $q_e^{''}$ that need to be evaluated. That means, only 4 unknown variables, m_{11}, m_{13}, m_{22}, and $q_e^{''}$ appeared in equation (5.26). The frequency location of transmission zero, ω in equation (5.26) can be controlled and set to a value. We have successfully reduced the 12 full solutions in equation (4.29) to 4 solutions through the mathematical analysis described. This has a benefit of reducing the computation time during the optimisation process. By optimisation, we meant minimising the function expression in equation (5.26). To do this, optimisation process has to be implemented to generate optimal values of the normalised coupling coefficients and external quality factors so that the given function in equation (5.26) is minimised. This is explained in the next section. An optimisation algorithm used and the iteration process carried out to design trisection filter is also presented in the next section.

5.2.2. Optimisation

Different techniques of optimisation have been utilized to synthesise coupled resonator filters. One of these techniques is based on optimisation of the normalised coupling coefficients in a normalised coupling matrix. The main advantage of coupling matrix optimisation technique is that it requires considerably less computational time than full scale EM simulations to complete the synthesis [8]. In this work, to realise a trisection filter, coupling matrix optimisation technique is used to obtain the coupling coefficients and the external quality factors in equation (5.26). Thus, equation (5.26) can be used as a cost function when using optimisation. The cost function in equation (5.26) is provided as

a function of 4 control variables (normalised coupling coefficients and external quality factors).

We have used an optimisation algorithm that uses unconstrained control variables to un-bound the search space so as to make a direct search starting from the initial guess. This is known as local optimisation algorithms. Local optimisation algorithms strongly depend on the initial values of the control parameters. The initial guess should be given as an input to the algorithm that seeks a local minimum within the local neighbourhood of the initial guess.

Initial values of control variables are guessed and provided. During optimisation process, a number of iterations will be performed to modify the variables so as to minimise the overall value of the function expression in equation (5.26). The iteration process will continue till an optimal solution that minimises the cost function is found.

5.2.2.1 Design Examples

A useful optimization method (solving a set of non-linear equation in (5.26) in Matlab® R2010B) is applied to the cost function in equation 5.26. The control variables in the optimisation algorithm are:

$$\{m_{11},\ m_{13},\ m_{22},\ q_e^{''}\}$$

Because the initial values in the optimization method depend on its convergence, the appropriate values have to be chosen. First of all, the initial control variables are guessed and systematically re-arranged putting the negative couplings into consideration. That is, before operating the optimization, the values are adjusted by comparing between the sign

of the control variables. The optimised normalised coupling parameters (or control variables) and the number of iterations performed by an optimiser along with the final errors are tabulated in table 5.2. The corresponding goal of return loss, RL in dB, at each stage of optimisation performed is included in the table 5.2.

Table 5.2: Optimised normalised coupling coefficients and external quality factors

m_{11}	m_{13}	m_{22}	$q_e^{"}$	Iterations	Error	Goal RL (dB)
0.0486	0.2287	-0.2467	1.0544	159	2.6621×10^{-10}	-14.28
0.0623	0.1394	-0.1246	1.2091	155	2.6595×10^{-9}	-13.7
-0.1470	-0.5491	0.4787	0.6699	49	4.8282×10^{-10}	-20.0
-0.0974	-0.3919	0.3794	0.8556	43	1.3583×10^{-10}	-25.0
-0.0974	-0.3919	0.3794	0.8556	39	1.3583×10^{-10}	-30.0

For each optimised normalised coupling coefficients and external quality factors, an asymmetric frequency response of trisection filter are examined and shown in figures 5.12 to 5.17 along with their normalised coupling matrices, $[m]$. It is evident from table 5.2 that a systematic selection and arrangement of initial control variables improves the number of iterations performed by an optimizer. That is, with a minimised function expression in equation (5.26), the optimised normalised control variables converge to

optimal values as shown in table 5.2. There are also improvements in the frequency responses as shown in figures 5.12 to 5.16.

$$m = \begin{bmatrix} 0.0486 & 0.9266 & 0.2287 \\ 0.9266 & -0.2467 & 0.9266 \\ 0.2287 & 0.9266 & 0.0486 \end{bmatrix}$$

$$q_{e1} = 0.9484 = q_{e2}$$

(a)

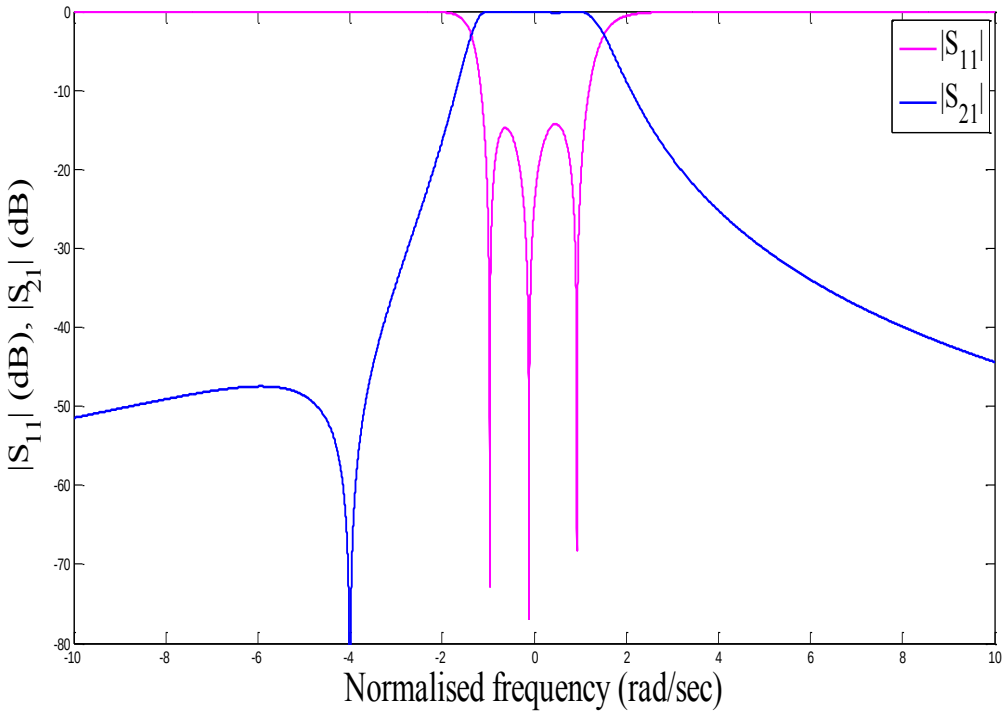

(b)

Figure 5. 12 (a) normalised coupling matrix and external quality factors and (b) response of trisection filter with a return loss of 14.28 dB.

$$m = \begin{bmatrix} 0.0572 & 0.9374 & 0.2348 \\ 0.9374 & -0.2578 & 0.9374 \\ 0.2348 & 0.9374 & 0.0572 \end{bmatrix},$$

$$q_{e1} = 0.9441 = q_{e2}$$

(a)

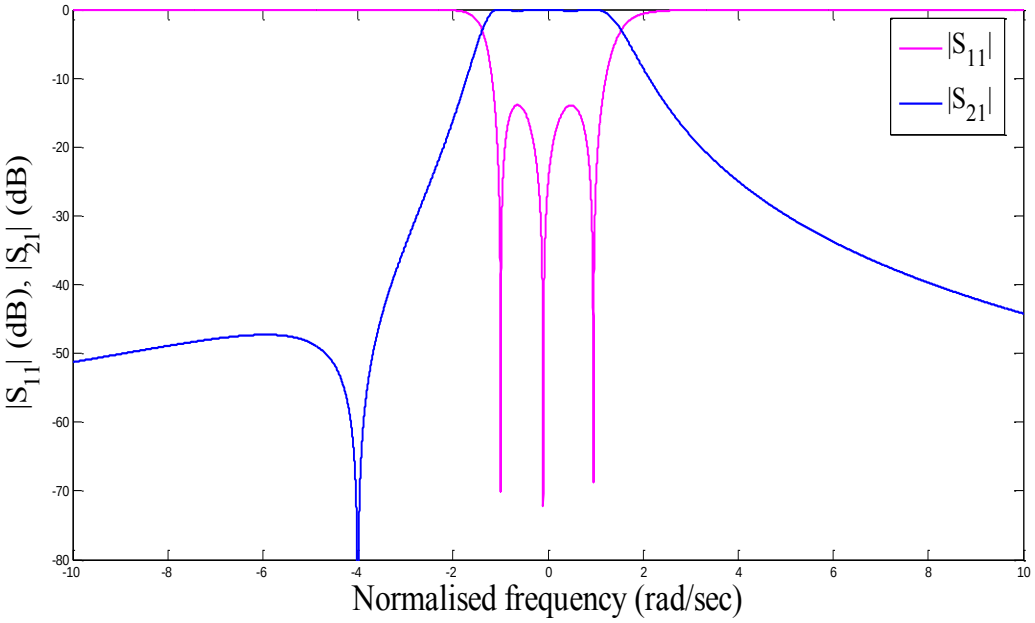

(b)

Figure 5. 13 (a) normalised coupling matrix and external quality factors and (b) response of trisection filter with a return loss of 13.7dB.

$$m = \begin{bmatrix} 0.0974 & -0.9740 & 0.3919 \\ -0.9740 & -0.3794 & -0.9740 \\ 0.3919 & -0.9740 & 0.0974 \end{bmatrix}$$

$$q_{e1} = q_{e2} = 0.8555$$

(a)

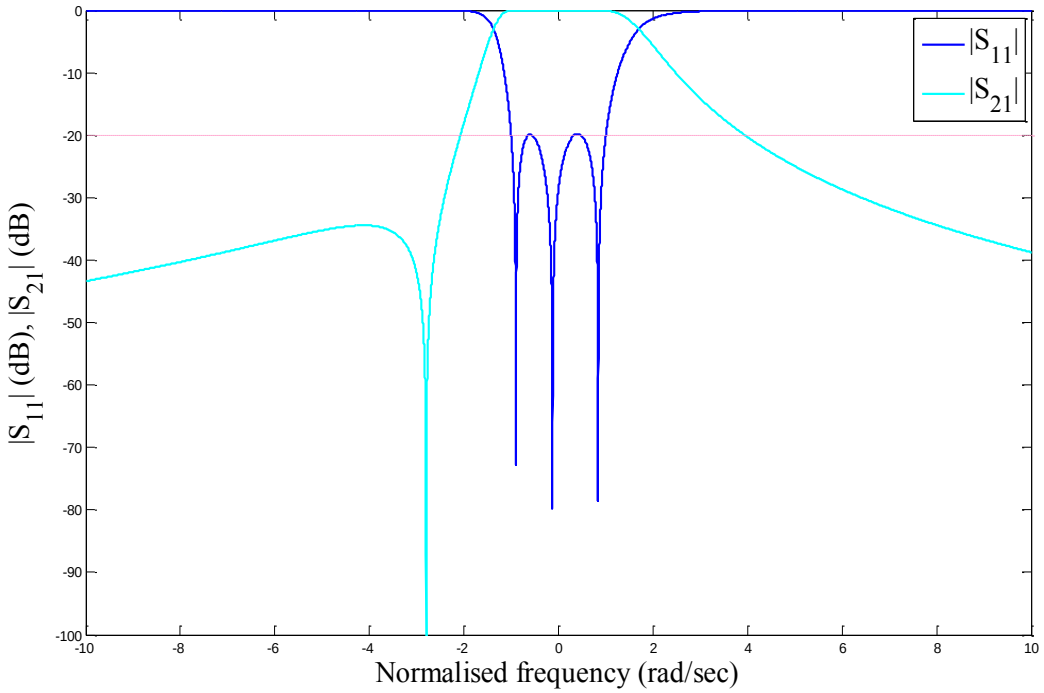

(b)

Figure 5. 14 (a) normalised coupling matrix and (b) response of trisection filter with a return loss of 20 dB.

$$m = \begin{bmatrix} -0.1470 & 1.1290 & -0.5491 \\ 1.1290 & 0.4787 & 1.1290 \\ -0.5491 & 1.1290 & -0.1470 \end{bmatrix}$$

$$q_{e1} = q_{e2} = 0.6699$$

(a)

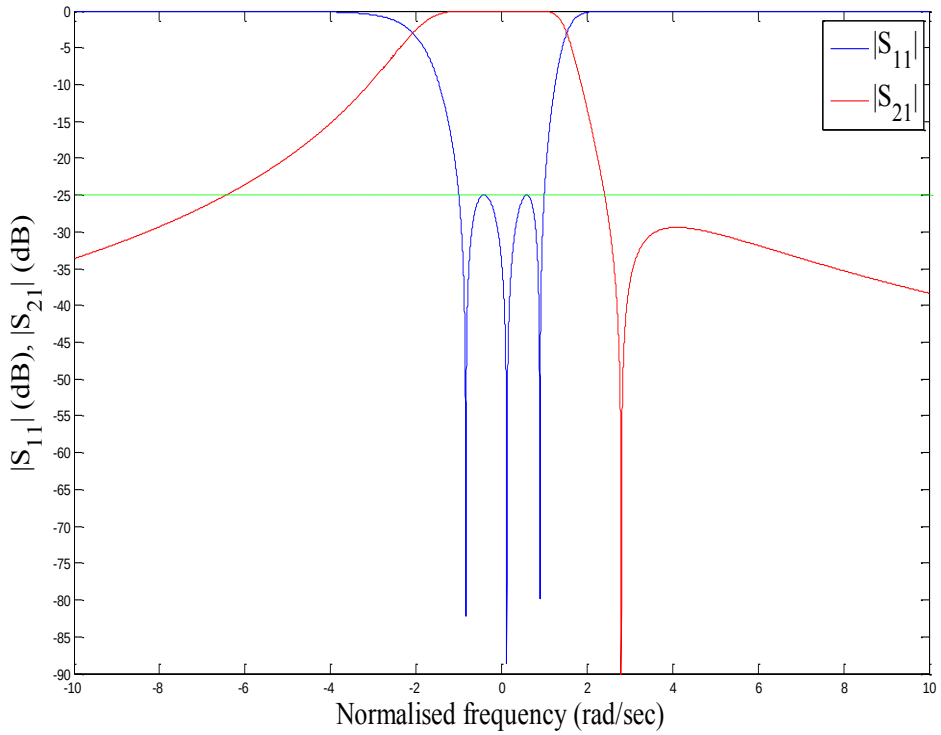

(b)

Figure 5. 15 (a) Normalised coupling matrix and external quality factors

(b) Response of trisection filter with a return loss of 25 dB.

$$m = \begin{bmatrix} 0.1713 & 1.3667 & 0.5995 \\ 1.3667 & -0.4843 & 1.3667 \\ 0.5995 & 1.3667 & 0.1713 \end{bmatrix}$$

$$q_{e1} = q_{e2} = 0.5354$$

(a)

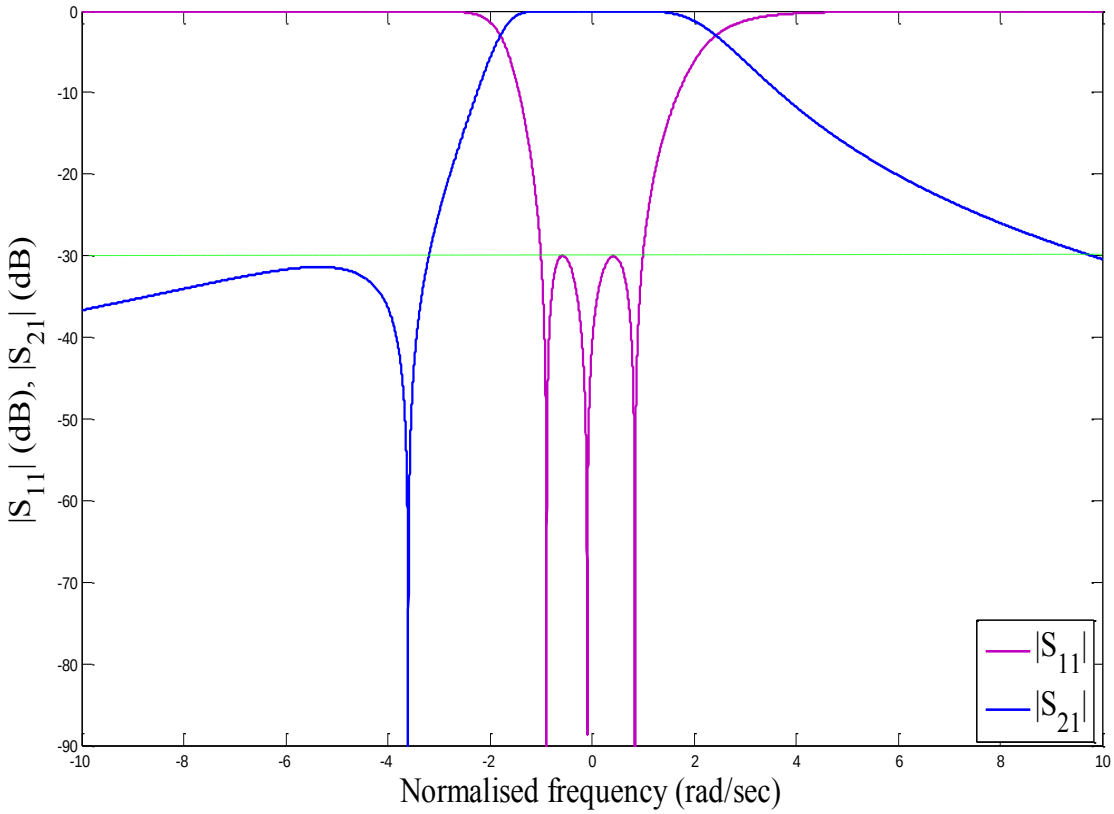

(b)

Figure 5. 16 (a) Normalised coupling matrix and external quality factors

(b) Response of trisection filter with a return loss of 30 dB.

It has been mentioned in previous section that the placement of transmission zero of a trisection filter is decided by the polarity of cross coupling between resonators 1 and 3. This has been realised throughout the trisection filter responses shown in figures 5.12 to 5.16. That is, if the cross coupling is positive, that is $m_{13}>0$, the attenuation pole of finite frequency is on the high frequency side of the passband, whereas if the cross coupling is negative, that is $m_{13}<0$, the attenuation pole of finite frequency is on the low side of passband. That means, an image frequency response is obtained by reversing the sign of

the normalised coupling coefficients as illustrated in the asymmetric frequency response graphs. This is of dual benefit given the possibility of designing the filter with the image frequency response directly from the original coupling matrix simply by reversing their signs.

Chapter 6

Conclusion and Future Work

6.1. Conclusion

An equivalent three-port circuit model for the tri-resonator filter including the coupling between the input and the output ports has been proposed. Based on this circuit, the general 3×3 coupling matrix of a 3-port network with only 3 resonators has been derived. Electric and magnetic couplings have been considered in the derivation, and a combined formula has been generalised for both types of coupling. Based on this unified solution, the transmission zero locations for S_{21} and S_{31} has been analytically proved and demonstrated.

Mathematical expressions have been derived to calculate the normalised coupling coefficients and external quality factors. The derivations of equations have been carried out without the use of conventional polynomial equations shown in equations 4.14 and 4.15. To avoid complexity of mathematical analysis, the three locations of reflection zeros for the proposed structure have been specified. The mathematical manipulations to derive the analytical formula for the computation of normalised coupling matrix and external quality factors have been based on the specified reflection zero locations.

With the aid of the general formulae, the normalised coupling coefficients and external quality factors have been calculated. Using these values, the 3-dB tri-resonator power splitter has been designed. The splitter response has reflection zeros at $-j$ and j, and this is consistent with the specified values of reflection zero locations as expected.

The thesis has presented a generalized synthesis method for tri-resonator filter structures. The mathematical relationship between the normalised coupling matrix and external quality factors has been given for the straight forward application of this new method. The normalised external quality factors and the return loss are mathematically related and graphically presented to have a better understanding of their relations. The graph of external quality factor versus return loss were found to be very important in getting particular values of normalised external quality factors at a particular return loss without doing any calculations.

A clear synthesis procedure for the design of 3-dB tri-resonator power splitter has been outlined, so that element values of coupling coefficients and external quality factors would be calculated to design 3-dB tri-resonator power splitter. This synthesis method has been applied to the symmetric 3-port network with two reflection zeros and infinite transmission zero. It is interesting to note that various ranges of coupling coefficients and external quality factors give rise to the same 3-dB power splitter as demonstrated in the practical design of a 3-dB tri-resonator power splitter.

The general formulae, which have been developed in this new synthesis method, are applied to the tri-coupled trisection filter having three reflection zeros and single transmission zero. From the general formulae, a simple mathematical function with a minimum number of control variables has been derived. The analytical function developed is optimised to fully realise the trisection filter. In doing so, the minimum iteration is achieved as the original control variables are reduced from 12 full solutions to 4. This obviously reduces the time taken during optimisation process. In this case, an achievement is attained in reducing the total control variables to a minimum.

Using the normalised optimised values of the control variables, an asymmetric frequency response of a trisection filter at different transmission zero locations has been realised. The transmission zero location for the trisection filter has not been included in the control variables as it is possible to control by varying its frequency locations, and finding its suitable place near the passband.

Similar to the 3-dB power splitter, various ranges of normalised coupling coefficients and external quality factors have been obtained for the trisection filter during optimisation. In the optimisation algorithm the initial values of control variables have been provided before the start of optimisation. Systematic selections and re-arrangements of initial control variables were found to be vital to get optimal values of control variables as shown in table 5.2

An image frequency response is examined by simply changing the sign of the cross coupling, m_{13}, between resonator 1 and 3, giving rise to design flexibility of the trisection filter.

The limitation of the new method described in this thesis is that it may not be applicable for higher order filters as the calculation will be clearly very complicated. As the order of the filter increases, mathematical analysis may become extremely intricate, time consuming, difficult to realise, and in some cases even impossible to perform.

6.2. Future Work

The work on power splitter design can be further implemented for coupled resonators using four or more resonators. In a three-port network structure, increasing the number of coupled resonators give rise to more reflection zeros. Thus, for a power-splitter with four

or more resonators coupled to one another, there may be more reflection zeros, and this may be further investigated. Further work can also be conducted on asymmetrical power splitter by using only three resonators.

The new analytic synthesis method introduced in this thesis may be used to realise a coupled resonator diplexer using only three resonators. Hence, further work on coupled resonators for a diplexer design may be conducted.

The design procedure outlined in this thesis for a tri-coupled tri-resonator power splitter can be employed as a basis for a three-port power splitter using four or more coupled resonators. Polynomial synthesis method for the two port network may also be adopted to three port networks to realise a power splitter when the number of coupled resonators within the structure increase.

The level of complexity of mathematical analysis to calculate coupling coefficients and external quality factors increase as the number of coupled resonator within a given structure increase. Thus, efficient optimisation techniques and algorithms are required to get entries of the coupling matrices.

References

[1] J. S. Hong and M. J. Lancaster, Microstrip filters for RF/Microwave applications, John Wiley and Sons, 2001

[2] T. Skaik, M. Lancaster, and F. Huang, "Coupled-Resonator 3-dB Power Divider", *Proceedings of the IET seminar on Passive RF and Microwave Components*, Birmingham, UK, April 2010, pp. 21-36.

[3] Robert S. Elliot, *An introduction to Guided Waves and microwave circuits,* Prentic-Hall, Inc. A Simon & Schuster Company, 1993.

[4] Kai Chang and Lung-Hwa Hsieh, *Microwave Ring Circuits and Related Structures*, Second Edition, John Wiley & Sons, Inc., Publication, 2004.

[5] I.Wolff and N. Knoppik, "Microstrip ring resonator and dispersion measurements on microstrip lines," *Electron. Lett*.,Vol. 7, No. 26, pp. 779–781, December 30, 1971.

[6] R.E. Collin, *Foundations for Microwave Engineering*. 2nd edition, John Wiley & Sons, 2001.

[7] David M. Pozar, *Microwave Engineering*, 3rd edition, John Wiley & Sons, 2005.

[8] Talal F. Skaik, Synthesis of Coupled Resonator Circuits with Multiple Outputs using Coupling Matrix Optimization, P.hD thesis, University of Birmingham, UK, 2011.

[9] Samuel Y.Liao, *Microwave devices and Circiuts,* Prentic-Hall, Inc., Englewood Cliffs, N.J, 1980.

[10] Kurzrok, R. M. "General Three-Resonator Filters in Waveguide", IEEE Transactions on Microwave Theory and Techniques, vol. 14, January 1966, pp. 46-47.

[11] A. Garcia-Lamperez, M. Salazar-Palma, and T.K. Sarkar, "Analytical synthesis of microwave multiport networks", IEEE MTT-S International Microwave symposium digests vol. 2, pp. 455-458, 2004.

[12] A.B. Jayyousi, and M.J. Lancaster, "A gradient-based optimization technique employing determinants for the synthesis of microwave coupled filters," IEEE , MTT- S International Microwave Symposium, USA, vol. 3, pp. 1369-1372, June, 2004.

[13] Giuseppe Macchiarella and Stefano Tamiazzo, "Novel Approach to the Synthesis of Microwave Diplexers", IEEE Transactions on Microwave theory and techniques, vol.54, No. 12, December 2006, 4281.

[14] Sanghoon Shin and Sridhar Kanamaluru, "Diplexer design using EM and circuit simulation Techniques", IEE microwave magazine, 1527-3342, pp., 77-82, April 2007.

[15] C. C. Yu and K. Chang, "Transmission-line analysis of a capacitively couple microstrip-ring resonator," IEEE Trans. Microwave Theory Tech., Vol. 45, No. 11, pp. 2018–2024, November 1997.

[16] H.I. Thal. Jr., "Design of microwave filters with arbitrary responses", Int. J. Microwave Millimetre-Wave CAE, vol. 7, no. 3, pp. 208–221, 1997.

[17] R.J. Cameron, "Advanced coupling matrix synthesis techniques for microwave Filters," IEEE Trans. Microwave Theory Tech., vol. 51, No. 1, January 2003, pp.1-10

[18] Richard J. Cameron, "General Coupling Matrix Synthesis Methods for Chebyshev Filtering Functions", *IEEE Transactions on Microwave theory and techniques*", vol. No. 47, vol. 47, No. 4, April 1999.

[19] Walid A. Atia, Kawthar Zaki and Ali E. Atia, "Synthesis of General Topology: Multiple Coupled Resonator Filters by optimization", *IEEE-Digest* PP. 821- 824, 1998

[20] Matthieu Kowalski, Emmanuel Vincent "Beyond the Narrowband Approximation: Wideband Convex Methods for Under-Determined Reverberant Audio Source Separation" *IEEE Transactions on Audio, Speech, and Language Processing* 18,7 (2010) pp. 1818 – 1829

[21] P. Troughton, "Measurement technique in microstrip", *Electron. Lett.*, Vol. 5, No. 2, pp. 25–26, January 23, 1969.

[22] K. Chang, F. Hsu, J. Berenz and K. Nakano, "Find optimum substrate thickness for Millimetre Wave GaAs MMICs," *Microwaves & RF*, Vol. 27, pp. 123–128, September 1984.

[23] W. Hoefer and A. Chattopadhyay, "Evaluation of the equivalent circuit parameters of microstrip discontinuities through perturbation of a resonant ring", *IEEE Trans. Microwave Theory Tech.*,Vol. MTT-23, pp. 1067–1071, December 1975.

[24] I.Wolff and N. Knoppik, "Microstrip ring resonator and dispersion measurements on microstrip lines", *Electron. Lett.*, Vol. 7, No. 26, pp. 779–781, December 30, 1971.

[25] S. Kanamaluru, M. Li, J. M. Carroll, J. M. Phillips, D. G. Naugle, and K. Chang, "Slotline ring resonator test method for high-Tc superconducting films", *IEEE Trans. App. Supercond*., Vol. ASC-4, No. 3, pp. 183–187, September 1994.

[26] K. Chang, T. S. Martin, F.Wang, and J. L. Klein, "On the study of microstrip ring and varactor-tuned ring circuits", *IEEE Trans. Microwave Theory Tech.*, Vol. MTT- 35, pp. 1288–1295, December 1987.

[27] L. Zhu and K.Wu, "A joint field/circuit model of line-to-ring coupling structures and its application to the design of microstrip dual-mode filters and ring resonator circuits" , *IEEE Trans. Microwave Theory Tech*., Vol. 47, No. 10, pp. 1938–1948, October 1999.

[28] H.I. Thal. Jr., "Computer aided filter alignment and diagnosis", IEEE Trans, Microwave Theory Tech., vol. MTT-26, pp. 958-963, December 1978.

[29] Robert J. Weber, "Introduction to Microwave Circuits: Radio Frequency and Design Applications", January 2001, Wiley-IEEE Press

[30] Richard J. Cameron, Chandra M. Kudsia and Raafat R. Mansour, "Microwave filters for communication systems, fundamentals, design and applications", 2nd edition, John Wiley & Sons, 2007

[31] D. Swanson, "Narrow-band microwave filter design", IEEE Microwave Magazine, 8:105-114, 2007.

[32] R. Hopkins and C. Free, "Equivalent circuit for the microstrip ring resonator suitable for broadband materials characterisation", IET, 2008.

[33] Lung-Hwa Hsieh, "Equivalent Lumped Elements G, L, C, and Unloaded Q's of Closed- and Open-Loop Ring Resonators", *Student Member, IEEE,* and Kai Chang, *IEE,* IEEE Transactions on Microwave theory and techniques, vol. No. 2, February 2002 .

Appendix A

Solution to Polynomial Equation

The cubic equation given, $f(p) = p^3 + ap^2 + bp + c = 0$ is significantly more difficult to solve than the quadratic equation, and cannot reasonably be written without a change of variables. However, we do not go for hand calculations to find the solutions of the cubic equation shown. We have introduced a simple math lab syntax called "sym" to calculate the zeros of the polynomial function. Sym is the Short-cut for constructing symbolic objects.

Each input argument must begin with a letter and must contain only alphanumeric characters to solve the polynomials using mat lab program. The solution for the cubic equation is provided as

```
Syms  a b c p;

solve('p^3+a*p^2+b*p+c');
```

p_1=

```
((a*b)/6 - c/2 + ((b/3 - a^2/9)^3 + (a^3/27 - (b*a)/6 + c/2)^2)^(1/2) - a^3/27)^(1/3) - (b/3 -
a^2/9)/((a*b)/6 - c/2 + ((b/3 - a^2/9)^3 + (a^3/27 - (b*a)/6 + c/2)^2)^(1/2) - a^3/27)^(1/3)
- a/3
```

P_2=

(b/3 - a^2/9)/(2*((a*b)/6 - c/2 + ((b/3 - a^2/9)^3 + (a^3/27 - (b*a)/6 + c/2)^2)^(1/2) - a^3/27)^(1/3)) - a/3 - ((a*b)/6 - c/2 + ((b/3 - a^2/9)^3 + (a^3/27 - (b*a)/6 + c/2)^2)^(1/2) - a^3/27)^(1/3)/2 - (3^(1/2)*i*((b/3 - a^2/9)/((a*b)/6 - c/2 + ((b/3 - a^2/9)^3 + (a^3/27 - (b*a)/6 + c/2)^2)^(1/2) - a^3/27)^(1/3) + ((a*b)/6 - c/2 + ((b/3 - a^2/9)^3 + (a^3/27 - (b*a)/6 + c/2)^2)^(1/2) - a^3/27)^(1/3)))/2

P_3=

(b/3 - a^2/9)/(2*((a*b)/6 - c/2 + ((b/3 - a^2/9)^3 + (a^3/27 - (b*a)/6 + c/2)^2)^(1/2) - a^3/27)^(1/3)) - a/3 - ((a*b)/6 - c/2 + ((b/3 - a^2/9)^3 + (a^3/27 - (b*a)/6 + c/2)^2)^(1/2) - a^3/27)^(1/3)/2 + (3^(1/2)*i*((b/3 - a^2/9)/((a*b)/6 - c/2 + ((b/3 - a^2/9)^3 + (a^3/27 - (b*a)/6 + c/2)^2)^(1/2) - a^3/27)^(1/3) + ((a*b)/6 - c/2 + ((b/3 - a^2/9)^3 + (a^3/27 - (b*a)/6 + c/2)^2)^(1/2) - a^3/27)^(1/3)))/2

Appendix B

Calculations of Cofactors and Determinant of the Normalised Coupling Matrix, $[A]$

The normalised coupling matrix, $[A]$, is given by

$$[A]=\begin{bmatrix} -jm_{11}+p+\dfrac{1}{q_{e1}} & -jm_{12} & -jm_{13} \\ -jm_{12} & -jm_{22}+p+\dfrac{1}{q_{e2}} & -jm_{23} \\ -jm_{13} & -jm_{23} & -jm_{33}+p+\dfrac{1}{q_{e3}} \end{bmatrix}$$

1. $cof_{12}\left(\left[A(p)\right]\right)$

The cofactor, $cof_{12}\left(\left[A(p)\right]\right)$ can be obtained by cancelling the first row and second column of matrix, $[A]$, and this is shown as

$$cof_{12}([A])=(-1)^{(i+j)}\begin{vmatrix} -jm_{12} & -jm_{13} \\ -jm_{23} & -jm_{33}+p+\dfrac{1}{q_{e3}} \end{vmatrix}$$

where i is a row number and j is a column number.

For this particular case $i=1$ and $j=2$. Thus

$$cof_{12}\left(\left[A(p)\right]\right) = -\left(-jm_{12}\left(-jm_{33}+p+\frac{1}{q_{e3}}\right)+m_{13}m_{23}\right)$$

$$= -(jm_{12}jm_{33} - jm_{12}p - jm_{12}.\frac{1}{q_{e3}} + m_{13}m_{23})$$

$$= m_{12}m_{33} + jm_{12}p + jm_{12}\frac{1}{q_{e3}} - m_{13}m_{23}$$

2. $\underline{cof_{13}\left(\left[A(p)\right]\right)}$

Similarly $Cof_{13}\left(\left[A(p)\right]\right)$ may be calculated by cancelling the first row and the third column of matrix, $\left[A\right]$, and this yields

$$cof_{13}\left(\left[A(p)\right]\right) = (-1)^{(i+j)}\begin{vmatrix} -jm_{12} & -jm_{13} \\ -jm_{22}+p+\frac{1}{q_{e2}} & -jm_{23} \end{vmatrix}$$

where $i=1$ is the first row, and $j=3$ is the third column of matrix, $\left[A\right]$. Thus

$$cof_{13}\left(\left[A(p)\right]\right) = -m_{12}m_{23} - (-jm_{13}(-jm_{22}+p+\frac{1}{q_{e2}}))$$

$$= -m_{12}m_{23} - (-jm_{13}(-jm_{22}+p+\frac{1}{q_{e2}}))$$

$$= -m_{12}m_{23} - (-jm_{13}(-jm_{22}+p+\frac{1}{q_{e2}}))$$

3. $cof_{11}\left(\left[A\right]\right)$

The cofactor, $cof_{11}\left(\left[A(p)\right]\right)$ may be also computed by cancelling the first row and the first column of matrix, $\left[A\right]$. This is shown as

$$cof_{11}\left(\left[A(p)\right]\right) = (-1)^{(i+j)}\begin{vmatrix} -jm_{22} + p + \dfrac{1}{q_{e2}} & -jm_{23} \\ -jm_{23} & -jm_{33} + p + \dfrac{1}{q_{e3}} \end{vmatrix}$$

where $i = j = 1$ is the first row and column of matrix, $\left[A\right]$.

Thus

$$cof_{11}\left(\left[A(p)\right]\right) = -m_{22}m_{33} - jm_{22}p - j\frac{m_{22}}{q_{e3}} - jm_{33}p + p^2 + \frac{p}{q_{e3}} - j\frac{m_{33}}{q_{e2}} +$$

$$\frac{p}{q_{e2}} + \frac{1}{q_{e2}q_{e3}} + (m_{23})^2$$

$$= p^2 + (\frac{1}{q_{e3}} + \frac{1}{q_{e2}} - jm_{22} - jm_{33})p + \frac{1}{q_{e2}q_{e3}} - m_{22}m_{33} +$$

$$(m_{23})^2 - j\frac{m_{22}}{q_{e3}} - j\frac{m_{33}}{q_{e2}}$$

4. $\det\left[A(p)\right]$

The determinant, $\det\left[A(p)\right]$ of the matrix, $\left[A\right]$ is calculated as

$$\det\left[A(p)\right] = (-jm_{11} + \frac{1}{q_{e1}} + p).\begin{vmatrix} -jm_{22} + p + \frac{1}{q_{e2}} & -jm_{23} \\ -jm_{23} & -jm_{33} + p + \frac{1}{q_{e3}} \end{vmatrix} +$$

$$jm_{12}.\begin{vmatrix} -jm_{12} & -jm_{23} \\ -jm_{13} & -jm_{33} + p + \frac{1}{q_{e3}} \end{vmatrix} - jm_{13}.\begin{vmatrix} -jm_{12} & -jm_{22} + p + \frac{1}{q_{e2}} \\ -jm_{13} & -jm_{23} \end{vmatrix}$$

$$\det\left[A(p)\right] = (-jm_{11} + \frac{1}{q_{e1}} + p)\left[\left(-jm_{22} + p + \frac{1}{q_{e2}}\right).\left(-jm_{33} + p + \frac{1}{q_{e3}}\right) - \left(-jm_{23}(-jm_{23})\right)\right] +$$

$$jm_{12}\left[-jm_{12}\left(-jm_{33} + p + \frac{1}{q_{e3}}\right) - \left(-jm_{13}(-jm_{23})\right)\right] -$$

$$jm_{13}\left[\left(-jm_{12}(-jm_{23})\right) + -jm_{13}\left(-jm_{22} + p + \frac{1}{q_{e2}}\right)\right]$$

$$= (-jm_{11} + \frac{1}{q_{e1}} + p)\begin{pmatrix} -m_{22}m_{33} - jm_{22}p - \frac{jm_{22}}{q_{e3}} - jm_{33}p + p^2 + \\ \frac{p}{q_{e3}} - \frac{jm_{33}}{q_{e2}} + \frac{p}{q_{e2}} + \frac{1}{q_{e2}q_{e3}} + (m_{23})^2 \end{pmatrix}$$

$$+ jm_{12}\left(-m_{12}m_{33} - jm_{12}p - \frac{jm_{12}}{q_{e3}} + m_{13}m_{23}\right) -$$

$$jm_{13}\left(-m_{12}m_{23} + m_{13}m_{22} + jm_{13}p + \frac{jm_{13}}{q_{e2}}\right)$$

$$\det\left[A(p)\right] = jm_{11}m_{22}m_{33} - m_{11}m_{22}p - \frac{m_{11}m_{22}}{q_{e3}} - m_{11}m_{33}p - jm_{11}p^2 - \frac{jm_{11}p}{q_{e3}} -$$

$$\frac{m_{11}m_{33}}{q_{e2}} - \frac{jm_{11}p}{q_{e2}} - \frac{jm_{11}}{q_{e2}q_{e3}} - jm_{11}\left(m_{23}\right)^2 - \frac{m_{22}m_{33}}{q_{e1}} - \frac{jm_{22}p}{q_{e1}} -$$

$$\frac{jm_{22}}{q_{e1}q_{e3}} - \frac{jm_{33}p}{q_{e1}} + \frac{p^2}{q_{e1}} + \frac{p}{q_{e1}q_{e3}} - \frac{jm_{33}}{q_{e1}q_{e2}} + \frac{p}{q_{e1}q_{e2}} + \frac{1}{q_{e1}q_{e2}q_{e3}} +$$

$$\frac{\left(m_{23}\right)^2}{q_{e1}} - m_{22}m_{33}p - jm_{22}p^2 - \frac{jm_{22}p}{q_{e3}} - jm_{33}p^2 + p^3 + \frac{p^2}{q_{e3}} -$$

$$\frac{jm_{33}p}{q_{e2}} + \frac{p^2}{q_{e2}} + \frac{p}{q_{e2}q_{e3}} + p\left(m_{23}\right)^2 - j(m_{12})^2 m_{33} + (m_{12})^2 p +$$

$$\frac{(m_{12})^2}{q_{e3}} + j2m_{12}m_{13}m_{23} - j(m_{13})^2 m_{22} + (m_{13})^2 p + \frac{(m_{13})^2}{q_{e2}}$$

Thus, rearranging the equation above yields

$$\det\left[A(p)\right] = p^3 + \left(-jm_{11} + \frac{1}{q_{e1}} - jm_{22} - jm_{33} + \frac{1}{q_{e3}} + \frac{1}{q_{e2}}\right)p^2 +$$

$$\left(-m_{11}m_{22} - m_{11}m_{33} - \frac{jm_{11}}{q_{e3}} - \frac{jm_{11}}{q_{e2}} - \frac{jm_{22}}{q_{e1}} - \frac{jm_{33}}{q_{e1}} + \frac{1}{q_{e1}q_{e3}}\right)p +$$

$$\left(\frac{1}{q_{e1}q_{e2}} - m_{22}m_{33} - \frac{jm_{22}}{q_{e3}} - \frac{jm_{33}}{q_{e2}} + \frac{1}{q_{e2}q_{e3}} + \left(m_{23}\right)^2 + (m_{12})^2 + (m_{13})^2\right)p +$$

$$jm_{11}m_{22}m_{33} - \frac{m_{11}m_{22}}{q_{e3}} - \frac{m_{11}m_{33}}{q_{e2}} - \frac{jm_{11}}{q_{e2}q_{e3}} - jm_{11}\left(m_{23}\right)^2 - \frac{m_{22}m_{33}}{q_{e1}} -$$

$$\frac{jm_{22}}{q_{e1}q_{e3}} - \frac{jm_{33}}{q_{e1}q_{e2}} + \frac{1}{q_{e1}q_{e2}q_{e3}} + \frac{\left(m_{23}\right)^2}{q_{e1}} - j(m_{12})^2 m_{33} + \frac{(m_{12})^2}{q_{e3}} +$$

$$j2m_{12}m_{13}m_{23} - j(m_{13})^2 m_{22} + \frac{(m_{13})^2}{q_{e2}}$$